

國立臺灣大學理學院大氣科學研究所

碩士論文

Graduate Institute of Atmospheric Sciences

College of Science

National Taiwan University

Master Thesis

從陸地大氣交互作用熱點談北美中部大平原之灌溉效應

From Land-Atmosphere Coupling Hotspot
to Irrigation Impacts over the Great Plains

吳姿瑩

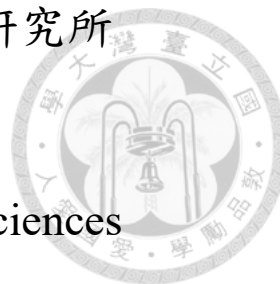
Tzu-Ying Wu

指導教授：羅敏輝 博士

Advisor: Min-Hui Lo, Ph. D.

中華民國一〇九年十一月

November, 2020



國立臺灣大學碩士學位論文 口試委員會審定書

本論文係 吳姿瑩君 (學號 R06229009) 在國立臺灣大學大氣科學學系、所完成之碩士學位論文，於民國 109 年 10 月 22 日承下列考試委員審查通過及口試及格，特此證明

口試委員：

羅 淑 輝 (簽名)

陳 奕 翰 (指導教授)

吳 珮 義

系主任、所長

游 政 谷 (簽名)

致謝



大約沒有想過自己可以走到這裡。碩班兩年半的時光，多半在躊躇忐忑與迷茫中度過，許多次說著要休學或延畢，但在終於有了一點研究突破後仍確定要延畢之時卻忽然悵然若失。過去的這些年，在認識自己的路上跌跌撞撞，已經快要遺忘那個會因為一個精彩的想法與理論而眼睛發光的女孩長得是什麼樣，然而現在終究把兒時願望給完結了，做出了一個屬於自己的研究。不論結果如何有限，也許未能把人們的知識疆域推前多少，但我盼望那個熱愛知識也渴望探究問題、把世界從點連成線再連成面的孩子還活在我心裡。

這本論文的誕生與完成，最要感謝羅敏輝老師的悉心指導、鼓勵與包容，實在難以想像還有哪個老師能這樣接納一個不成熟的學生。自從我推甄碩班寄給老師看研究計畫時，老師便展現了極大的支持與鼓勵。在我猶豫著是否繼續求學之時，甚至入學前先赴波蘭研習一年時，老師也欣於聽我分享在波蘭的生活。在我在八月底才遲遲返台選擇指導教授時，老師也一口答應收我。對於我頻繁地感到不踏實而自我懷疑的時候，老師總能樂觀、甚至在我看來過分樂觀地相信我：相信我能順利走過碩班的學業、相信我能勝任課程助教的工作、相信我能夠給出一個讓別人有收穫的報告、相信我能完成審查期刊文章的工作、相信我能在跨國研究計畫中有所貢獻(儘管最後我還是退出了)，相信我們能找到一個我在意也覺得舒服的題目，並且讓我們已知的事情再往前推進一點點。甚至在我畫錯圖的時候，老師也總是先相信我畫的是對的，才去找其他結果是否有不合理之處。在我被徬徨與焦慮淹沒的時候，逃避、拖延、壓死線甚至錯過死線成為常態，老師卻從未有過一句指責，總是以我的狀態為優先，其他的問題與責任則給他來扛。老師不僅給我空間找回自己的生活節奏，也在我不主動回報進度時定期關心我有沒有什麼想討論的，不是研究的事情也可以。

在研究上，老師也總是能在一團混亂的結果中看出有用的資訊與觀點，在我終於能把一系列研究連貫起來、想通資料與實驗之間的關聯時，老師也能一聽就理解我的推論，並且把我卡住的地方解開來，用一個看起來風馬牛不相及卻概念上相類似的觀點來重新詮釋，讓整個論證過程忽然變得有說服力。在老師的引導下，也慢慢讓我感覺很多文獻裡還沒能回答的事情並不是做不到、只是需要更多更仔細的實驗去驗證。做研究並不總是需要把因果關係混

澆才能為自己開脫，也不需要為資料戴上有色眼鏡、套入自己的敘事，而是可以讓資料自己說話。有位朋友曾跟我說，他從前不太想踏入量化研究的世界是因為擔心這樣每個人做出來的研究都會長得一樣，但是讓我放下質性研究、回到科學的初衷則是擔心研究者的眼光會干預你的判斷，反而你想看見什麼就能找到支持這套敘事的證據。總覺得喜歡做研究的人應該都有著一種寬廣的信仰：你能透過探究方方面面的知識來更認識這個世界。如果緊抓著既有的認知不放，那恐怕你抓住的也不會是真知灼見。然而在這趟對於知識與學術抱有某種固執的旅途上，我也慢慢發現即便是量化研究，每個人也都會讓自己的題目長成不同的模樣。非常感激羅老師陪伴我走過了這段路，容許我的無愧於心需要透過一個這麼糾結的過程才能達到，也讓這份研究最終能以一個更完整的樣子呈現在世人面前。雖然仍有諸多不足，但我相信至少我已做到誠實。

另外感謝莊振義與陳奕穎兩位老師願意擔任我的口試委員，也感謝洪景山老師溫暖而熱心地回應我的來信邀約。在陸地大氣交互作用與氣候預報的研究上我還只是個生澀的學徒，有許多研究的環節還沒能處理得完善，但感謝兩位老師和善而敏銳地提點幾個重要的問題，讓我能夠以更好的方式重新表述或加以思考，雖然最終文稿沒能完全納入這些延伸的課題與討論，但這些問題對於我釐清這個課題仍有許多幫助。在認識如何做研究的這條道路上，我亦十分感謝帶我淺嚐研究的謝志豪老師，不僅讓我見識到處理問題要如何抽絲剝繭、去追問這些分析建立在什麼假設上，並且在探究的過程中發展出一套看待問題的框架，同時也讓我意識到學無止盡，我們不可能什麼都準備好才開始去做研究，你只能做中學然後在過程中慢慢裝備好自己，同時不同資料有其適合回答的問題，不要期待同一組資料能為你解答所有問題。那個夏天也讓我見識到聰明的人又是多麼努力，跟 420 的大家一起成長的過程非常愉快，謝謝梵絃在研究上的指導，小至操作浮游生物實驗、如何撰寫工作日誌，大至研究方向的擬定，謝謝 Ester、Mini、匡庭在統計方法上的幫忙與研究上的鼓勵與陪伴，謝謝貞儀與俊偉在非線性科學與 coding 上的指點，謝謝佳君、政喻與治甫一起完成這個不容易的挑戰。這段時間從撰寫每天的工作日誌，到學習整理文獻、依不同類別訂閱各大期刊的 RSS，到旁聽實驗室讀書會，都是紮實到難忘的訓練。也十分感謝郭鴻基老師因為跟謝志豪老師有合作關係而對我印象深刻，謝謝老師對我能力的肯定，在我大二那年主動問我有沒有出國念書的打算，

表示想要推薦我去加州大學爾灣分校，但是基於我對如何面對知識仍有困惑，還沒準備好投入研究工作中，也不敢賠上老師的信用，於是婉言拒絕了。直到今天我仍然無法確認自己是否有他人所說的那種潛力，也不後悔當初拒絕了老師難得的推薦，能夠誠實面對自己、堅持本心從來都是更重要的事。也謝謝已故的林清涼老師對一個懵懂無知的高一小女生苦口婆心叮嚀基礎功的重要性並且不要追逐流行的課題，曾雪峰老師鼓勵我想做什麼就能去做，對於我惶惑茫然在國家圖書館搜索拼湊到的課題並未展示出任何輕慢，反而說我準備好隨時都可以去找他討論。謝謝諸多高中科學研習社及友社的學長姐，難以一一列舉，但特別想謝謝那年夏天狠狠打臉我說我還停留在收集資料的階段而不是自己去設定假說、設計實驗的學長，謝謝每次社課後留下來一兩個小時解答我的問題的學長姐，謝謝在聽完我的海報後給予鼓勵並分享中研院天文所大幅海報給我的高選昀學長，謝謝曹一允與呂行學長在我在社團發問了不成熟的問題後仍願意指點我並帶我到臺大校園找教授聊聊，一允之後在國外攻讀博班的日子裡也給了我很多做研究上的建言與心理調適的過來人分享。謝謝朱希平學長在聯合社課後不定期的關心與問候，在我對自己的能力失去信心時給予最堅實的肯定與鼓勵。謝謝讓我能初到大氣系時不感到害怕，還能加入許多課程討論與課外活動的大氣系同學、學長姐、學弟妹，謝謝你們讓我這樣孤僻的人能夠在一個陌生的環境不感到孤單，並且在缺乏各種大氣系所必要的技能下還能蒙混過關。

謝謝讓我在大一什麼都不懂的狀況下就進實驗室的李清勝老師，謝謝颱風實驗室的旭峰學長、魚丸學長、秀妮學姐、阿其學長、人璋學姐、心誠學姐、竟豪學長，讓我這個大一沒修大氣科學概論的人也能慢慢認識大氣系的人在關心什麼、都看哪些教科書、使用些什麼程式語言，甚至都去哪裡吃飯。謝謝陳維婷與陳正平老師讓我在大三的時候有機會到紐約州立大學阿爾巴尼分校參訪一個月，對於一個從未自己出國的人來說是非常讓人興奮且充滿啟發的一次經驗。不敢說在大氣科學智識的進展有多少，但開始認識到在大氣科學可以做的事情很多，如同楊明仁老師在回程路上同我所說的：大氣科學需要各式各樣的人，你一定有自己可以做的事情。也非常感謝啟芸學姐在我在 Albany 期間的熱心協助，不僅協助我安頓下來，幫我向別人借用桌子、還幫我搬上房間，帶我去各大超市與百貨逛街，一起吃飯聊天的那段時光非常難忘。也謝謝台灣學生會的怡人、Ariel、Donna、William 在 Albany 期間的幫忙與各種

活動的籌備，謝謝 Kenneth 對我的文字的喜歡並鼓勵我繼續寫，謝謝 Tracy 跟我分享你的部落格。另外也謝謝因為暑期計畫而認識的炫慶與昭誠，在紐約一起到處玩的時光是我人生中最快樂的日子之一。也謝謝 Cidny，雖然當時還不太熟，但很開心你之後還回到臺大來攻讀學位，我們才有更進一步認識的契機，一起陪伴彼此度過煎熬的研究生生活。謝謝大氣系的老師們，其中特別感謝陳正平老師對我碩論研究的關注並給予寶貴的意見，謝謝盧孟明老師在氣候變異與預測課程上的悉心指導，不僅讓我在大氣所修習的第一門課就能快速掌握氣候學界的知識與術語，也對我與碩論掛勾的課程報告有著高度的興趣與期待，謝謝洪惠敏老師從大學以來對我這樣不務正業的學生的鼓勵與支持，在我還不確定要往哪裡走的時候，在波蘭政府獎學金申請截止的前一個禮拜毫不猶豫地應允幫我寫推薦信，並給我切實的職涯建議，謝謝黃彥婷老師永遠熱情溫暖的笑容，在我從波蘭剛回來的時候第一個在氣候論壇上見到的就是黃老師了，也是氣候動力與全球變遷實驗室讓我感覺原來大氣系沒有忘記我，原來我還是可以回到這個像家一樣的地方。

還要特別感謝陸地水文氣候實驗室以及 C404 的大家。身為一個不擅與人互動之人，能夠這樣平平安安地、只需要顧及自己內在的漩渦，實在仰賴這世界的善意以及他人的負重前行。謝謝榮佑學長在處理 CESM 模式上的幫忙，謝謝小傑學長不厭其煩地回答我關於研究的各種疑難雜症，最近幾個月一起練跑的時光也讓我慢慢開始相信自己有能力完成一些目標，謝謝庭慧在研究上的互相支持，有人可以一起討論研究還有氣候模式的種種麻煩真的是件讓人安心的事，也謝謝你讓台灣杉包機計畫運行順利。也謝謝鶴鳴、晉輝、鎔與、譯心、玉蓮、博元、鈺湄、晏寧、珮軒、淳弘、子瑩在研究上的討論與交流。另外特別感謝嘉偉學長在水氣收支平衡方程上的協助還有研究上的意見，謝謝淇雅在研究上的大力幫忙，不僅事隔兩年還時常被我打攪當年碩論的各種問題，也給了我的研究很多重要的提醒。謝謝每次海報競賽給予珍貴意見與討論的匿名委員，也非常謝謝開治與王珩在 AGU 的時候遠道來聽我還非常不知所云的海報，並給了我許多新鮮的刺激與想法。還要特別感謝好同學元懷，雖然是超級厲害的神人還是非常謙虛，一起聊天的時光總能緩解在研究上的各種受挫。最後謝謝我的家人，我知道我一直以來是最讓人擔心的女兒，我會學著長大，也希望你們看得到。謝謝這些情份讓我能夠再撐著多走一哩路，然後是下一哩路。

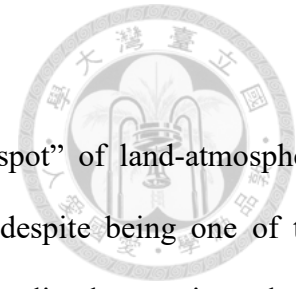
中文摘要



許多研究指出北美中部大平原為陸地大氣交互作用之熱點，並視其為改進季內尺度預報的重點區域。然而北美中部作為全球主要糧倉之一、每年灌溉用水量僅次於季風亞洲區，在過去文獻中灌溉對降水的反應卻相當分歧。這份研究旨在透過探討陸地大氣交互作用熱點的概念，試圖解釋灌溉對於當地降水影響不顯著的原因。GLACE (Global Land-Atmosphere Coupling Experiment) 是一組透過全球氣候模式來探討陸地大氣交互作用強度的系集實驗，其後多份研究利用這組實驗定義出陸地大氣交互作用熱點。由於 GLACE 移除陸地大氣交互作用的作法是在未耦合實驗裡強制給定耦合實驗的土壤濕度，這樣的研究方法將改變兩組實驗的土壤濕度變異度，反映陸地大氣交互作用熱點的定義是建立在該地對於土壤濕度變異度的敏感程度。我們因此推測灌溉對於北美中部降水的影響結果分歧，是因為不同研究中考慮灌溉的方式不同，使得土壤濕度的變異度有所差異所導致。我們使用與 GLACE 相同的全球氣候模式 CESM (Community Earth System Model) 來進行灌溉實驗，並採用兩種灌溉情境來改變土壤濕度的變異度：其一是透過注水讓土壤水飽和的方式直接改變土壤濕度，其二是透過將灌溉水均勻灑在表層土壤作為有效降水。結果顯示，雖然注水讓土壤水飽和的方式能夠有效增加表層土壤水，但其在增加蒸發散量的幅度反而不如噴灑灌溉來得大。這與 GLACE 所推論的結果不同，顯示在灌溉實驗中蒸發散量之變化不完全由土壤濕度變異度所主導。除此之外，雖然灌溉實驗中土壤濕度的增加能夠顯著增加蒸發散量，但降水反應卻不如 GLACE 所顯示的顯著，也就是說增加的蒸發散量並未能有效轉換成當地降水，這可能跟北美中部大平原的降水主要由中尺度對流系統所貢獻有關。值得注意的是，儘管夏季平均降水並未增多，但在注水讓土壤水飽和的實驗中卻可觀察到降水在年際尺度上變異度的下降，亦即灌溉活動可能讓乾年變得較濕、濕年變得較乾，因而灌溉實驗中的平均降水沒有太大的變化。這顯示了土壤濕度變異度之重要性。

關鍵字：陸地大氣交互作用、灌溉、水文氣候、土壤濕度變異度、北美中部大平原

ABSTRACT



The Great Plains in North America has been identified as a “hotspot” of land-atmosphere coupling, but shown equivocal responses in various irrigation studies despite being one of the breadbaskets in the world. In this study, the concept of land-atmosphere coupling hotspot is explored using GLACE (Global Land-Atmosphere Coupling Experiment). We assume that the diverged irrigation responses among the modeling studies can be explained by the differences in soil moisture variability resulting from different irrigation representations. To compare with GLACE, we adopted the same global climate model, Community Earth System Model (CESM), for our irrigation experiments. We considered two types of irrigation method (flood irrigation vs. sprinkler irrigation) and modified the irrigation water amount to assess whether the effect of soil moisture (SM) variability would be obscured by the mean SM differences. The results show that, although flood irrigation can remarkably increase soil moisture values, sprinkler irrigation is more effective in enhancing evapotranspiration (ET), implying that the changes in ET is not purely determined by soil moisture variability as GLACE suggests. In addition, despite the general increase in ET in the irrigation experiments, precipitation response is not as significant as GLACE indicates, which shows that the increase in ET cannot translate into local precipitation. Previous studies also have indicated that ET might not have a strong influence on precipitation in this region where the rainfall is primarily nocturnal induced by mesoscale convective systems. Notably, although the JJA mean precipitation does not vary much, precipitation variability reduces significantly where the soil moisture variability is reduced. That said, irrigation possibly makes dry years wetter and wet years drier, so that the mean precipitation changes little. This study underscores the importance of soil moisture variability changes.

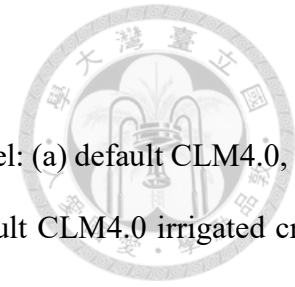
Keywords: land-atmosphere coupling, irrigation, hydroclimate, soil moisture variability, Great Plains in North America

CONTENTS



致謝.....	i
中文摘要.....	v
ABSTRACT.....	vi
CONTENTS.....	vii
LIST OF FIGURES	viii
LIST OF TABLES	xi
Chapter 1 Introduction	1
Chapter 2 Data and Method	8
2.1 GLACE Experiment.....	8
2.2 Land-atmosphere Coupling Metrics.....	10
2.3 CESM1 Irrigation Experiments	11
2.4 Interannual Comparison between Irrigation and Control simulations.....	14
Chapter 3 Results	18
3.1 Inference from GLACE Experiment.....	18
3.2 Effect of Irrigation Prescriptions.....	19
Chapter 4 Summary and Discussion	30
Chapter 5 Future work	36
REFERENCE.....	40

LIST OF FIGURES



- Figure 2-1** Prescribed irrigated C3 crop fraction in the land model: (a) default CLM4.0, (b) SMSat and (c) SMSat_more. SMSat irrigates over the default CLM4.0 irrigated crop fraction, with the remainder rain-fed crop fractions. SMSat_more irrigates over the entire crop fractions, where the rain-fed crop fractions are set to be zero. Both experiments restrict the irrigated crop only over the grid cells specified in central North America (indicated as the red box). 15
- Figure 2-2** Intensive irrigated areas over the Great Plains identified by grid box encompassing: (a) monthly mean irrigation water within range of 10^0 and 10^2 mm from Wada and Bierkens (2014) averaged over 1960-2014; (b) irrigated crop fraction over 30% in CLM4.0 surface dataset. 16
- Figure 2-3** Irrigation rate (mm/month) for four irrigation experiments: (a) seasonal cycle averaged over 2001-2014, (b) spatial distribution of climatology JJA mean. The shading indicates the specified irrigated areas. The legend of (a) indicates the JJA climatology sum of each irrigation experiment. 17
- Figure 3-1** GLACE-style land-atmosphere coupling metric for (a) precipitation and (b) evapotranspiration (ET) variability in boreal summer (JJA) using 10 ensemble members over 1971-2014. The red box indicated the irrigated areas specified for the irrigation experiments. Note that the coupling hotspot distribution is sensitive to the timespan and the ensemble members chosen. 21
- Figure 3-2** Effect of land-atmosphere coupling on soil moisture and evapotranspiration (SM-ET) correlations for ensemble mean in JJA from 1981-2014. 22
- Figure 3-3** Effect of land-atmosphere coupling on SM-ET distribution for ensemble mean in JJA over the Great Plains (indicated in Figure 3-2), using (a) land-standalone (LAND) simulations, and (b) LA-coupled ATM simulations only. The darker dots of

(a) indicate LA-uncoupled runs compared to LA-coupled runs. Gray dots in (b) shows the individual month of JJA for each year from 1981 to 2014. The green dots of (b) are the top and bottom 7% soil moisture in the probability distribution, which have equally the same average soil moisture values as the blue dots (see also Table 3-1).²³

Figure 3-4 Effect of land-atmosphere coupling on distribution of monthly JJA (a) root zone soil moisture, (b) ET and (d) precipitation for the ensemble mean over the Great Plains. The y axis shows histogram densities. The legend indicates the coupled or uncoupled, land-atmosphere coupled or land-only set of simulations used for the corresponding variables. ATM simulations were used for atmospheric variables such as precipitation whereas LAND simulations for land surface variables such as soil moisture and ET. Here we present soil moisture distribution from ATM simulations to show the JJA soil moisture values from LA-uncoupled ATM were held fixed from the climatology of JJA LA-coupled ATM.²⁴

Figure 3-5 Effect of different irrigation prescriptions on distribution of monthly JJA root zone soil moisture, ET and precipitation in the Great Plains over the 20-year simulations: SMSat, SMrain, SMSat_more, SMrain_more. The y axis is histogram densities. The legend compares the control run with the irrigation run for each experiment. The vertical dashed line indicates the mean of control run, and the solid line indicates the mean of irrigation run. The units are mm/month.²⁵

Figure 3-6 Effect of different irrigation prescriptions on SM-ET relationship using JJA monthly values over the 20-year simulations over the Great Plains. The blue dots indicate experiments using soil saturation (mimic flood irrigation) while the green dots indicate experiments using effective rain rate (mimic sprinkler irrigation). The gray line represents the Budyko curve and distinguishes the three hydrological regimes.²⁶

Figure 3-7 Distribution of SM-ET, SM-P and SM-ET for their JJA interannual standard deviation (a-c) and JJA climatology mean (d-f) over the Great Plains. The darker dots

indicate data points from GLACE while the lighter dots indicate data points from irrigation experiments. The regression lines are computed only by data from irrigation experiments. * indicate significance level greater than 95% and ** indicate significance level greater than 99%.27

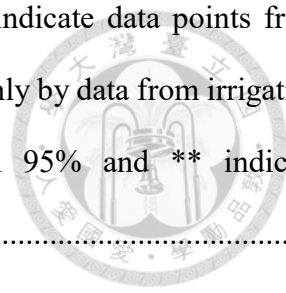


Figure 3-8 Interannual variation of irrigation-induced precipitation (mm/month) among the irrigation experiments over the Great Plains in JJA. The blue-tone dots are flood irrigation experiments, whereas the orange-tone dots are sprinkler irrigation experiments.29

Figure 3-9 Vertical profile of divergence field over the Great Plains in JJA for each set of experiments. The blue solid line is the ensemble mean of LA-coupled simulations from GLACE, while the green dashed line is the ensemble mean of LA-uncoupled simulations. The remainder are from irrigation experiments.....29

Figure 4-1 Vertical profile of divergence field over the Great Plains in JJA for two irrigation prescriptions in dry and wet years. The darker lines indicate the dry years while lighter lines are the wet years. The blue (orange)-tone lines are flood (sprinkler) irrigation experiments. The gray lines indicate control runs.34

Figure 4-2 Diurnal cycle of total precipitation over the Great Plains for control simulations and irrigation runs in unit of mm/hr. The black solid line indicates control run while the blue dashed shows the irrigation-induced rainfall changes. SMonce is similar to SMSat with the top1m soil moisture set to field capacity once per day.35

Figure 5-1 Variation of groundwater table depth over time for the irrigation experiments in the Great Plains over the course of simulation years.39

LIST OF TABLES

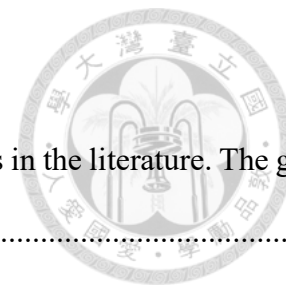


Table 1-1 Comparison of irrigation impacts over the Great Plains in the literature. The gray shading indicates modeling studies.....	5
Table 1-2 Comparison between irrigation methods in modeling studies.	7
Table 2-1 Model configurations for GLACE-Hydrology and irrigation experiments. The section of GLACE is the Table 1 in Kumar et al. (2020).....	12
Table 2-2 CESM1 irrigation experiment settings.....	14
Table 3-1 Comparison between JJA ET from dry- and wet-side soil moisture and ET from moderate soil moisture in LA-coupled ATM simulations averaged over the Great Plains. Units are mm/month.....	23
Table 3-2 Mean and standard deviation of JJA monthly soil moisture, ET and precipitation for GLACE and irrigation experiments, respectively. The standard deviation indicates interannual variability where JJA are averaged to remove intraseasonal variation. LAND simulations were used for soil moisture and ET in the GLACE experiment. The grids are averaged over the smaller box. Units: mm/month.....	28
Table 4-1 Variance decomposition of mean JJA precipitation for each year averaged over the Great Plains for the irrigation experiments. P indicates precipitation, and D indicates vertical-integrated divergence. The units for the variance are mm ²	34
Table 4-2 Coefficient of determination (R^2) for JJA mean precipitation-evapotranspiration (P-ET) and precipitation-divergence (P-D) relationship in the Great Plains over the 20-year simulations using the simple linear regression model.	35
Table 5-1 Same as Table 3-2, but included another SMrain experiment which irrigated over a larger extent (denoted as SMrain').	38
Table 5-2 Similar to Table 5-1, but the grids were averaged over the large box (red box indicated in Figure 2-1).....	38

Chapter 1 Introduction

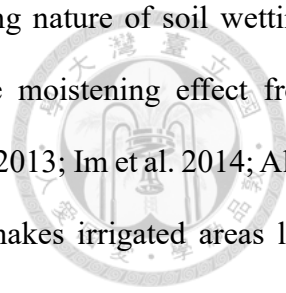
While the better representation of land surface conditions has been widely recognized to provide additional subseasonal to seasonal predictability (e.g., Koster et al. 2004, 2010, 2011; Douville 2010; Guo et al. 2011; Peings et al. 2011; Mahanama et al. 2012; Orsolini et al. 2013; Hirsch et al. 2014; Kumar et al. 2014; Materia et al. 2014; Koster and Walker 2015; Prodhomme et al. 2016; Thomas et al. 2016; Ceglar et al. 2018; Halder et al. 2018; Li et al. 2019), the interpretation and implications of land-atmosphere coupling hotspots are yet to be elucidated.

For instance, a drier and wetter soil moisture condition do not have equal effects on atmospheric predictability. Wetter land surface states in central North America are found to have higher temperature (Kumar et al. 2014) and precipitation (Schubert et al. 2008) predictability, while dry soil moisture anomalies have been found to provide higher skill in regions with wet climates (Koster et al. 2011). Guo and Dirmeyer (2013) further found that land-atmosphere coupling strength is enhanced over dry (wet) climate regions such as the Great Plains and Sahel (northern India) during wet (dry) years, suggesting that the strength of the coupling and/or predictability is highly sensitive to evaporative regime (McDermid et al. 2019): only when the soil moisture values enter into the intermediate ranges, the land surface has stronger impacts on surface fluxes and convection. However, it remains obscure whether this effect only takes place over coupling hotspot regions since another study (Wei and Dirmeyer 2012) showed that the stronger soil moisture-evapotranspiration (SM-ET) relation, which is a precursor of land-atmosphere coupling (Guo et al. 2006), also appears in the very dry regions of North Africa, the Middle East, and the Gobi Desert during wet months. Note that the changes in predictability do not necessarily have the same sign as the predictability itself, given our land surface memory is biased towards the dry conditions. A dry soil moisture anomaly can persist longer than a wet soil moisture anomaly (Kim and Wang 2012), and our predictive skill of a drought event is generally higher than that of a pluvial one (Quesada et al. 2012; Kumar et al. 2020).

Although Schubert et al. (2008) concluded that the changes in predictability in their AGCM

(Atmospheric General Circulation Model) simulations are primarily driven by changes in land-atmosphere coupling strengths, some studies pointed out that the increase in land-atmosphere coupling strength cannot guarantee the increase in precipitation predictability. Kumar et al. (2020) showed that the enhanced SM-ET relation from land-atmosphere coupling does not transfer to precipitation predictability. Likewise, Dirmeyer et al. (2013) showed that the predictability driven by land surface changes does not increase with land-atmosphere coupling strength under warming scenarios.

In addition, the Great Plains in North America, identified as one of the most robust coupling hotspots across various models and modeling studies such as GLACE-style multimodel intercomparison projects, has shown equivocal responses of local precipitation to irrigation (Schickedanz 1976; Barnston and Schickedanz 1984; Segal et al. 1998; Moore and Rojstaczer 2001; DeAngelis et al. 2010; Harding and Snyder 2012; Huber et al. 2014; Alter et al. 2015; Pei et al. 2016; Lu et al. 2017). As one of the breadbaskets in North America, the Great Plains is heavily reliant on irrigation water supply for its continental climate with low precipitation. By 1990, around 20 000 million m³ of groundwater has been added to the Great Plains annually, and the irrigated land areas have been expanded to 60 000 km² (Moore and Rojstaczer 2001). This groundwater pumping also has resulted in average declines of 3.9 m in water table depth between predevelopment and 2005 (McGuire 2007; Harding and Snyder 2012). It is therefore counterintuitive to see such considerable soil moistening to have disparate effects on the atmosphere, especially in a land-atmosphere coupling hotspot region. Welty and Zeng (2018) attempted to resolve this problem by showing that the positive soil moisture-precipitation (SM-P) relation only appears in high dynamic regimes (i.e. when the vertically-integrated moisture convergence is strong), which is aligned with the finding that irrigation can only amplify the preexisting rainfall areas but may not be able to produce strong uplifts to trigger convective systems (Schickedanz 1976; Segal et al. 1998; Harding and Snyder 2012; Huber et al. 2014). However, Welty and Zeng (2018) still failed to explain why the correlation becomes markedly insignificant when all regime days were considered.



Some studies approached this problem by considering the contrasting nature of soil wetting: surface cooling from evaporation and reduced net radiation versus the moistening effect from increased atmospheric humidity (DeAngelis et al. 2010; Lo and Famiglietti 2013; Im et al. 2014; Alter et al. 2015b; Lu et al. 2017). They proposed that the surface cooling makes irrigated areas less favorable for convection to occur and that irrigation-induced precipitation primarily occurs on the downwind side. Lu et al. (2017) interpreted the insignificant or reduced rainfall as evidence of the negative effect of irrigation on land-atmosphere coupling strength, which measures the atmospheric response to the land surface changes (Dirmeyer et al. 2012, 2014). Since land-atmosphere interactions are reciprocal, it is arguable to give only one side of the story. Specifically speaking, the land-atmosphere coupling metrics are not stationary: irrigation modifies the land surface states, the exchange in turbulent heat fluxes, and thereby changes in precipitation and land-driven potential predictability. The atmospheric responses would also feedback to the land surface and land-atmosphere interactions, which is manifested in the coupling metrics. A common but fallible argument herein is that one can arbitrarily assign the cause and effect in the mutual causation system. While it is legitimate for Lu et al. (2017) to claim that the weakened coupling strength is a natural product of the reduced rainfall, one should keep in mind that the metric itself is changing. Similarly, while Cook et al. (2011) attempted to explain the reduced irrigation cooling under increased GHG forcing by the absence of precipitation increase, one should be aware that near-surface temperature can also impact regional circulation and precipitation, and that the reduced surface cooling might also result from inadequate irrigation rate relative to the increased evaporative demand followed by GHG warming.

Inspired by the GLACE experiment, we noticed that land-atmosphere coupling strengths are strongly dependent on soil moisture variability, which is also the land surface property that irrigation directly modulates. In essence, irrigation is invented to supply necessary soil water for crop growth and production, which by nature, decreases soil moisture variability and weakens the SM-ET relation. Just as the land-atmosphere decoupled simulations in GLACE turned off the feedbacks from the land surface to the atmosphere, irrigation may weaken the land-atmosphere interactions by diminishing

the capability for the land surface to respond. If we take a closer look at the irrigation-related papers focusing on the Great Plains (**Table 1-1**), one may find the diverse results in rainfall appear mostly in modeling studies, including increase (Segal et al. 1998; Puma and Cook 2010; Harding and Snyder 2012; Qian et al. 2013) , decrease (Pei et al. 2016; Lu et al. 2017), and no significant changes (Adegoke et al. 2003; Huber et al. 2014) despite the general increasing trend in observational studies. By showing that these modeling studies not only used different climate models but considered irrigation differently (**Table 1-2**), we hypothesize that the latter is an important source of this diverged irrigation response in precipitation. The purpose of this study is to dissect the concept of land-atmosphere coupling hotspots to explain why irrigation cannot take effect on the Great Plains. That said, we assume the diverged response among modeling studies can be explained by the differences in soil moisture variability resulting from different irrigation prescriptions. We also modified the amount of irrigation water withdrawal to assess whether the effect of soil moisture variability would be obscured by mean soil moisture differences.

Table 1-1 Comparison of irrigation impacts over the Great Plains in the literature. The gray shading indicates modeling studies.

Reference	Data	Resolution	Irrigation Representation	Analysis Period	Local Precipitation	Notes
Present Study	CESM1	0.9° x 1.25° Monthly	Held top 1m soil to field capacity for irrigated crop fraction (SMsat)	1976-1995	Increase (slight)	
			Held top 1m soil to field capacity for the entire crop fraction (SMsat_more)	1976-1995	Increase	
			Add to effective precipitation rate on topsoil (SMrain)	1976-1995	Increase	
			Add to effective precipitation rate on topsoil (SMrain_more)	1976-1995	Decrease	
Schickedanz (1976)	Gauge stations (NWS)	32km x 32km Monthly	Factor analysis of irrigated areas	1931-1970	Increase in J-J-A	N/A
Barnston et al. (1984)	Weather maps (NWS), Precip, TS, Pres (NCDC)	Daily	Same as Schickedanz (1976)	1931-1970	Increase in J-J	N/A
Segal et al. (1998)	MM5	90km x 90km 6-day	Prescribe ET rate during 0600-1800 LST	Normal (1984) Flood (1993) Drought (1988)	Increase in J-J	Convection amplification
Moore et al. (2001)	Gauge stations (NCDC)	Monthly	Same as Schickedanz (1976)	1948-1997	No significant changes	Slower irrigation expansion
DeAngelis et al. (2010)	Precip (NCDC; gridded), Wind (NARR)	1°x1° Monthly	Groundwater use trend; change point analysis for monthly	1900-2000 (Precipitation) 1985-2006 (Q, U, V)	Increase in July	N/A

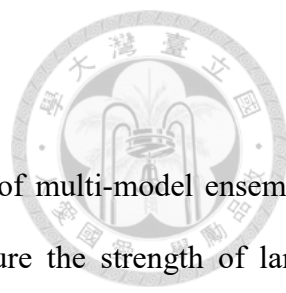
		rainfall; moisture tracking for high and low ET years				
Harding et al. (2012)	WRF-Noah	10km x 10km monthly	Apply water to soil surface to saturation for top 2m	Normal (1997, 1990, 1985) Pluvial (1993, 2008, 2007) Drought (1983, 2000, 1988)	Increase in normal, pluvial years	Nocturnal rainfall; convection amplification
Huber et al. (2014)	WRF-Noah	12km x 12km daily	Set top 1m soil to field capacity once a day	May-July (2001, normal)	No significant changes	Convection amplification
Alter et al. (2015)	Station (GHCND, Precipitation)	daily	Greatest precipitation intensity change occurred between 1950-1980 when irrigation rapidly intensified	1895-2011	Increased frequency in August; intensity and totals in J-A	Convection triggering
Pei et al. (2016)	WRF-Noah-Mosaic	30km x 30km monthly	Add to effective rain rate on topsoil for 2h at a rate of 20mm/h	J-J-A (2012, dry)	Decrease	Reduced sensible heating inhibited convection
Lu et al. (2017)	WRF-CLM4	50km x 50km daily	Add to effective rain rate on top of crop canopy at a rate of 0.72mm/h	2005	Decrease	N/A

Table 1-2 Comparison between irrigation methods in modeling studies.

Literature	Model	How to apply irrigation	When to trigger irrigation	Irrigated areas	Local Precipitation
Present Study	CESM1	Held at saturation for top 1m Add to effective rain rate (topsoil)	Throughout the day	1) Crop / Irrigated crop 2) Regardless of PFT	1) Increase 2) Increase (slight)
Segal et al. (1998)	MM5	Prescribe ET rate with daily total of 6mm (i.e. peak irrigation rate)	0600-1800 LST	Disaggregated from irrigation dataset	Increase
Adegoke et al. (2003)	RAMS	Saturated once daily for top 20cm	0000 UTC	Irrigated crop fraction	Insignificant
Puma and Cook (2010)	GISS ModelE	Add to effective rain rate (topsoil)	Throughout the day	Vegetated fraction	Increase
Harding et al. (2012)	WRF-Noah	Apply water to soil surface to saturation for top 2m	Throughout the day	Disaggregated from irrigation dataset	Increase
Qian et al. (2013)	WRF-Noah	Uniform rate from 0600-1000 LST (on top of crop canopy)	Greenness fraction above 40% of annual range 0600 LST: Root-zone moisture availability < 50% field capacity	Crop fraction; non-crop fractions if remaining water	Increase (slight)
Huber et al. (2014)	WRF-Noah	Saturated once daily for top 1m	0000 UTC	Entire grid cell containing any amount of irrigated land	Insignificant
Pei et al. (2016)	WRF-Noah-Mosaic	Add to effective rain rate (topsoil) for 2h at a rate of 20mm/h	10-40cm SM < (wilting point + 20% plant available water)	Irrigated crop and pasture	Decrease
Lu et al. (2017)	WRF-CLM4crop	Add with a rate of 0.72mm/h from groundwater on top of crop canopy	LAI > 0.1 m ² m ⁻² Root water stress < 0.99 or leaf temperature > 35°C	Disaggregated from irrigation dataset	Decrease

Chapter 2 Data and Method

2.1 GLACE Experiment



Global Land-Atmosphere Coupling Experiment (GLACE) is a pair of multi-model ensemble simulations first proposed by Koster et al. (2002) to objectively measure the strength of land-atmosphere coupling in AGCMs. This approach requires two sets of experiments: (1) the “W” ensemble (for “write” because the prognostic variable information is stored in a file) which is freely evolved with land and atmosphere segments interactively coupled, and (2) the “S” ensemble (modified from the R ensemble for “read in soil moisture” other than all land prognostic variables) in which the land-atmosphere coupling is muted by overwriting the soil moisture values saved from one of the W ensemble members in the deep root zone. In this regard, the S ensemble retains the *mean* effect of land-atmosphere interactions, while interrupting the additional feedback from the atmosphere. The difference in W and S ensembles in their intra-ensemble similarity is considered as an indicator of the strength of land-atmosphere coupling.

The GLACE experiment phase 1 (Koster 2004; Koster et al. 2006) has been extended for different research purposes, such as GLACE-2 (Koster et al. 2011), GLACE-CMIP5 (Seneviratne et al. 2013; Berg et al. 2014; Lorenz et al. 2016) and GLACE-Hydrology (Kumar et al. 2020). In this study, we used the model outputs from GLACE-Hydrology (Kumar et al. 2020), which is implemented in the Community Earth System Modeling Framework version 1.2.2 (CESM1.2.2, hereafter referred to as CESM1) (Hurrell et al. 2013). They performed 2 x 10-member ensemble experiments (with and without interactive soil moisture) with the observed sea surface temperature data from 1971-2014 as oceanic boundary conditions (Hurrell et al. 2008). The non-interactive simulations are performed by prescribing the climatological seasonal cycle of total soil water averaged over 1981-2014, for the first 10 years treated as a spin-up period. Then, the three-hourly atmospheric outputs from both sets of experiments were used to force the land-only ensemble simulations, allowing investigation of the resulting soil moisture variability under both the

W and S ensembles. Following Kumar et al. (2020), we referred the first-stage outputs as L-A coupled and L-A uncoupled ATM, and the second-stage outputs as L-A coupled and L-A uncoupled LAND. Since land-atmosphere coupling is generally stronger in summer (Dirmeyer 2003; Berg et al. 2014), our analysis focuses on the distribution of hotspot regions in boreal summer [June-July-August (JJA)]. In order to include the soil moisture variation in the subsurface, we considered top 1m soil moisture in our analysis, which is roughly the root zone depth for wheat, maize, and barley (Fan et al. 2016).

Aside from some modifications on model configurations for known biases, we would like to highlight a few key differences in the model setup between the GLACE-1 and GLACE-Hydrology for readers' reference. First, GLACE-1 control simulations correspond to one set of SST conditions (1994) but differing atmospheric conditions, whereas ensemble members of GLACE-Hydrology are forced by the same set of varying SSTs from AMIP simulations (Gates 1992) for historical period 1971-2014. While GLACE-1 removed the predictability associated with interannual SST variability, it may also lose accuracy in simulating the effect of oceanic processes on circulation changes and local precipitation recycling, given that rising temperature can raise the importance of oceanic evaporation for continental precipitation (Findell et al. 2019), albeit some studies (Koster et al. 2000) indicated a relatively weak SST impact in midlatitudes (encompassing the North American hotspot).

Second, GLACE-1 prescribed subsurface (effective depth more than 5 cm) soil moisture seasonal cycle by transient outputs from one ensemble member of the interactive runs for each timestep, while GLACE-Hydrology chose to specify soil moisture by its climatological values computed from the original coupled simulations. The use of climatological soil moisture values further creates some side-effects on the system (Seneviratne et al. 2006; Berg et al. 2014): (1) zero interannual variation of soil moisture, (2) a damped intra-annual variation of soil moisture, and (3) spurious latent heat source and precipitation increase over certain regions without soil moisture depletion. Comparing with GLACE-1, which only investigates the impact of zero inter-member differences, GLACE-Hydrology removes the interannual variability and allows the intra-annual variation and seasonal changes.

2.2 Land-atmosphere Coupling Metrics

We considered two coupling metrics: the GLACE type coupling strength parameters and the correlation between soil moisture and evapotranspiration (ET).

GLACE-type coupling strength parameters. To ensure we can reproduce the coupling hotspot map shown in Koster (2004), we computed the land-atmosphere coupling metric by the definition of Koster et al. (2002):

$$\Omega_p = \frac{N\sigma_{\hat{p}}^2 - \sigma_p^2}{(N-1)\sigma_p^2} \quad (2.1)$$

where N is the number of ensemble members, p denotes precipitation as the response of the atmosphere, σ is the standard deviation, and \hat{p} represents the ensemble mean; thus, $\sigma_{\hat{p}}$ is the standard deviation of the ensemble mean time series, and σ_p is the standard deviation of the time series from entire ensemble members. Here Ω_p measures the degree to which the individual time series of each ensemble member are similar, and the relative contribution of chaotic variability from the initial conditions to precipitation. The land-atmosphere coupling metric is then defined by

$$\Omega_p(S) - \Omega_p(W) \quad (2.2)$$

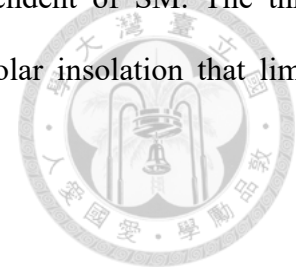
for the subtraction should isolate the impact of prescribed soil moisture values on precipitation. We also considered the metric for the land segment, that is,

$$\Omega_E(S) - \Omega_E(W) \quad (2.3)$$

to identify the signature of land-atmosphere coupling on the near-surface field.

Relationship between SM and ET. This is a simple framework developed by Koster et al. (2009) and has shown to be akin to the β curve proposed by Budyko (1974) using the land surface model with a simple representation of ET (Manabe 1969, based on Budyko 1956; see also "first-generation schemes" in Sellers 1997 and "soil moisture-evapotranspiration coupling" in Seneviratne et al. 2010). The relationship between SM and ET distinguishes three different evaporative regimes: (1) the dry soil moisture regime where ET is almost zero, (2) the transitional soil moisture regime (also known as a soil-moisture-limited regime) where ET is proportional to SM, and (3) the wet soil moisture

regime (also known as an energy-limited regime) where ET is independent of SM. The three hydroclimate regimes differentiate whether it is the soil moisture or solar insolation that limits evapotranspiration.



2.3 CESM1 Irrigation Experiments

The irrigation experiments were performed for 1971-2000 with the atmosphere/land stand-alone configuration of CESM1.2.2 with a horizontal resolution of roughly $0.9^\circ \times 1.25^\circ$. We used the version of CAM5 and CLM4.0, which is slightly different from CLM4.5 using in the GLACE-Hydrology experiment. Nonetheless, according to the CLM45 documentation (Oleson et al. 2013), major revised parameterizations are to reduce biases of biogeochemical substances and products, including low carbon stocks and unrealistic low gross primary production (GPP) in the Arctic, excessive GPP and unrealistic high leaf area index (LAI) in the tropics. The updates to hydrological processes are more about frozen soils, which should have little effects on our analysis since we are focusing on midlatitudes and boreal summer. To isolate the irrigation impacts, we used climatology SSTs and aerosol concentrations from a temporal 20-year window surrounding year 2000 (Rasch et al. 2019) instead of the observed ones as GLACE-Hydrology to reduce interannual variability and maximize irrigation effects on climate. A comparison of model configurations between our irrigation experiments and GLACE-Hydrology is briefly summarized in **Table 2-1**.

Table 2-1 Model configurations for GLACE-Hydrology and irrigation experiments. The section of GLACE is the Table 1 in Kumar et al. (2020).



Exp. Type	Experiment ID	Soil moisture	Climate forcing	SST forcing
Atmosphere-Land	CTL, SMsat,		Interactive	Fixed SST surrounding year 2000
	SMsat_more, SMrain, SMrain_more	Interactive	atmosphere model (CAM5)	
AMIP Type	LA coupled ATM	Interactive	Interactive	Time evolving observed SST from 1971 to 2014
	LA uncoupled ATM	Prescribed	atmosphere model (CAM5)	
Land-only	LA coupled LAND	Interactive	LA coupled ATM	N/A
	LA uncoupled LAND	Interactive	LA uncoupled ATM	N/A


To further testify our hypothesis that the irrigation methods cause the diverged response in precipitation, we considered two types of irrigation prescription using the framework of CLM4.0 crop and irrigation model (Levis and Sacks 2011): flood irrigation and sprinkler irrigation. Although the sprinkler method is more dominant than surface irrigation (Maupin et al. 2014), we also considered flood irrigation in which soil moisture variability is more likely to be changed. We mimicked sprinkler irrigation by adding irrigation rate to effective precipitation on the top soil, bypassing canopy interception, over the entire grid cell specified over the Great Plains. The irrigation rate for each timestep is disaggregated from the monthly irrigation water dataset (Wada and Bierkens 2014). We prescribed the same 2001-2014 climatology for each simulation year to remove interannual variability for irrigation water use. On the other hand, we imitated flood irrigation by directly modifying soil moisture values to field capacity. Since this approach is doomed to consume much more water than reality, we adjusted the fraction of irrigated grid cells to ensure the irrigation water amount of the two approaches are comparable. The procedure of flood irrigation is described below.

When irrigation is enabled, the fraction of C3 generic crop of each grid cell is divided into irrigated and non-irrigated portion based on a dataset of areas equipped for irrigation (Siebert et al. 2007, 2015), where the fraction of total cropland area is determined according to the default CLM

dataset (Oleson KW et al. 2010). To remove the irrigation effects from other irrigated regions, we restricted irrigation to be implemented only over the Great Plains for the entire C3 crop fraction, then forced the irrigated C3 crop portion to be zero elsewhere (**Figure 2-1**). Specified irrigated areas were identified by monthly mean irrigation water over 1 mm/month averaged over 1960 to 2014 (**Figure 2-2a**), using a 5 arc-second observation-based, hydrological-model-driven global irrigation dataset (Wada and Bierkens 2014) which has been calibrated against national statistics from Food and Agriculture Organization of the United Nations (FAO). The chosen irrigated areas can also correspond to intensive irrigated crop fractions in CLM4.0 (**Figure 2-2b**). To ensure that the model only irrigates during the growing season, two criteria have to be satisfied: (1) the soils are not frozen; (2) the transpiration wetness factor falls below 1, that is, when the transpiration rate is less than the evaporation rate of a hypothetical water surface having the same temperature and exposure as the leaf (vanBavel et al. 1965), indicating the vegetation is growing. Once the two conditions are met, irrigation is triggered at the specific timing for each experiment. Note that although by definition flood irrigation approach does not allow the soil to be dried out, the soil moisture was replenished at the beginning of the model and gradually dried out as runoff or evapotranspiration in the simulating process. In this regard, the output soil moisture values would not be held fixed.

To further examine if the effect of soil moisture variability would be altered under different irrigation water amounts, we considered another set of irrigation experiment by increasing the irrigation rate in sprinkler irrigation and increasing the fraction of irrigated grid cell to entire C3 crop in flood irrigation. The seasonal cycle and irrigation spatial pattern for the four irrigation experiments are shown in **Figure 2-3**, where SMsat and SMsat_more indicate flood irrigation and SMrain and SMrain_more represent sprinkler irrigation. The irrigation experiment settings are briefly summarized in **Table 2-2**. Note that the irrigated areas for SMrain is much smaller than others for the different research purpose in the first instance. Therefore, the following analysis is based on the areal mean using the smaller grid box to avoid the dilution of irrigation impacts in the SMrain experiment.

Table 2-2 CESM1 irrigation experiment settings.

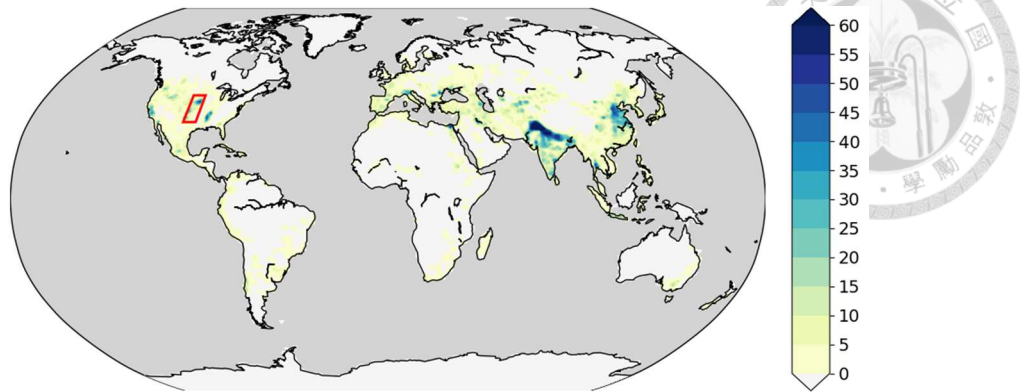


Casename	How to apply	When to trigger	Irrigation water amount
SMsat	Saturate top 1m SM	Throughout the day	Realistic
SMrain	Add effective rain rate		
SMsat_more	Saturate top 1m SM	Throughout the day	Hypothetical
SMrain_more	Add effective rain rate		

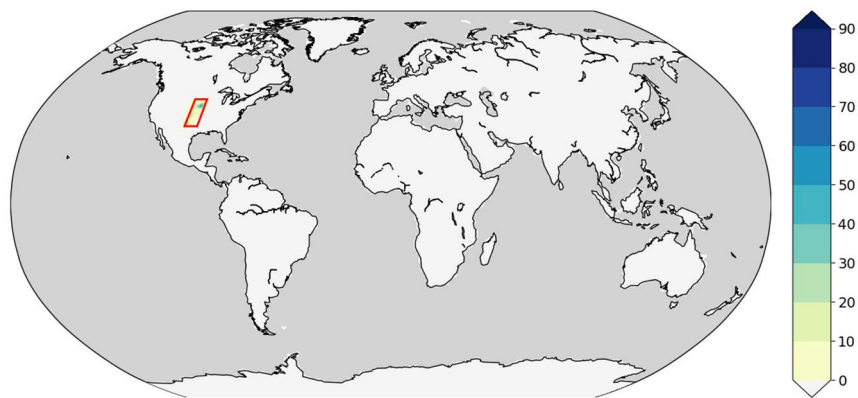
2.4 Interannual Comparison between Irrigation and Control simulations

Since the irrigation experiments were driven by climatological SST surrounding the year 2000 but not observational SST from the historical runs, one cannot treat the simulation year as the historical year. For instance, the year 25 in irrigation run cannot correspond to the year 25 in control run for each year is considered as an individual ensemble member. In this regard, the 20-year average is equivalent to the ensemble mean. Therefore, to compute the irrigation-induced changes in dry years and wet years, we cannot directly subtract the control run by the irrigation run for each year. In contrast, we calculated the difference between each irrigation year and a single wet (dry) year identified by control run. Since we have 20-year simulations for both irrigation and control runs, we would obtain 20 values for each wet and dry year, then the mean and standard deviation of these 20 years show the irrigation effects in that year.

(a) Irrigated crop fraction (%) in CLM4.0



(b) Irrigated crop fraction (%) in SMsat



(c) Irrigated crop fraction (%) in SMsat_more

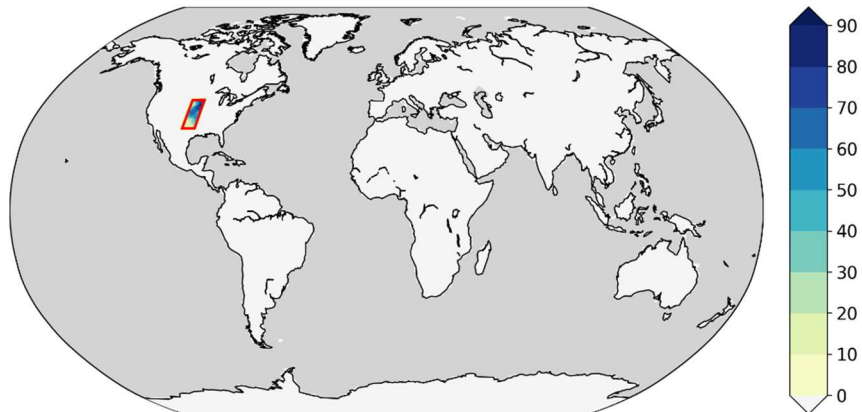
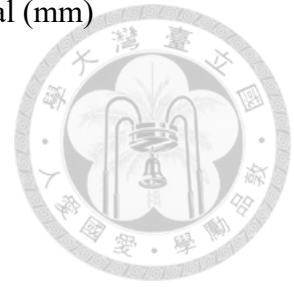
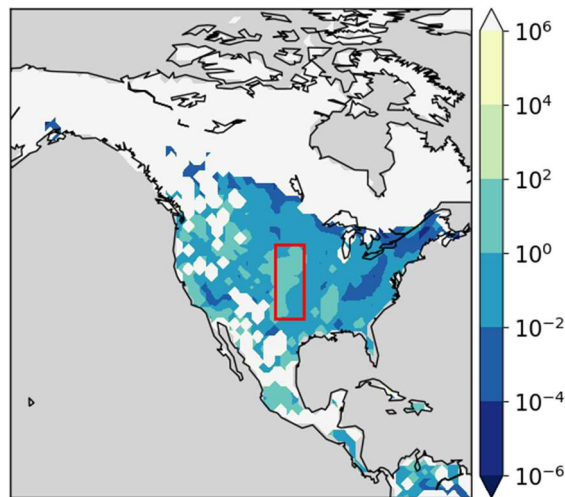


Figure 2-1 Prescribed irrigated C3 crop fraction in the land model: (a) default CLM4.0, (b) SMsat and (c) SMsat_more. SMsat irrigates over the default CLM4.0 irrigated crop fraction, with the remainder rain-fed crop fractions. SMsat_more irrigates over the entire crop fractions, where the rain-fed crop fractions are set to be zero. Both experiments restrict the irrigated crop only over the grid cells specified in central North America (indicated as the red box).

(a) Monthly mean irrigation water withdrawal (mm)



(b) Irrigated crop fraction (%) in CLM4.0

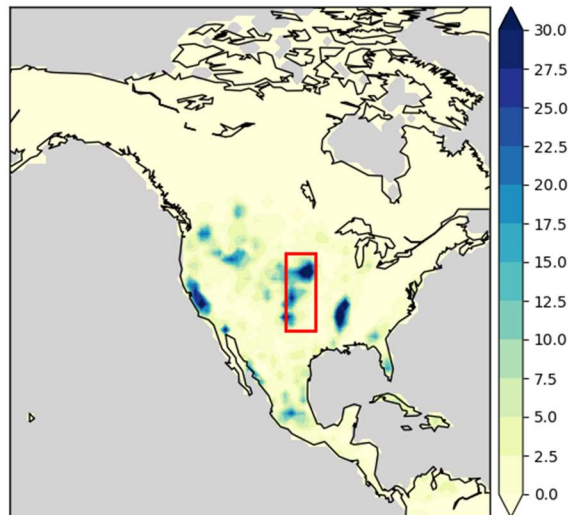
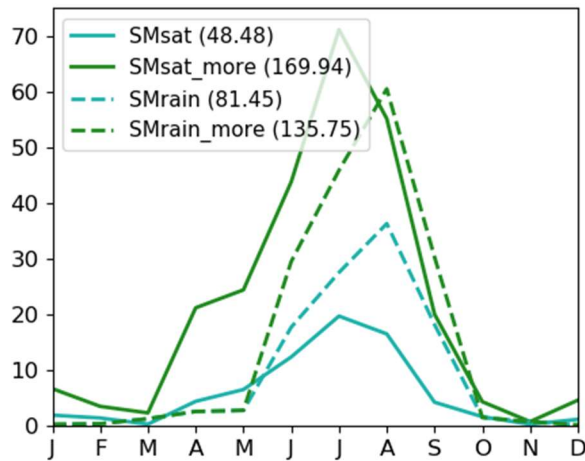


Figure 2-2 Intensive irrigated areas over the Great Plains identified by grid box encompassing: (a) monthly mean irrigation water within range of 10^0 and 10^2 mm from Wada and Bierkens (2014) averaged over 1960-2014; (b) irrigated crop fraction over 30% in CLM4.0 surface dataset.

(a) Seasonal cycle of irrigation rate (mm/month)



(b) Regional map of climatology irrigation rate (mm/month) for boreal summer

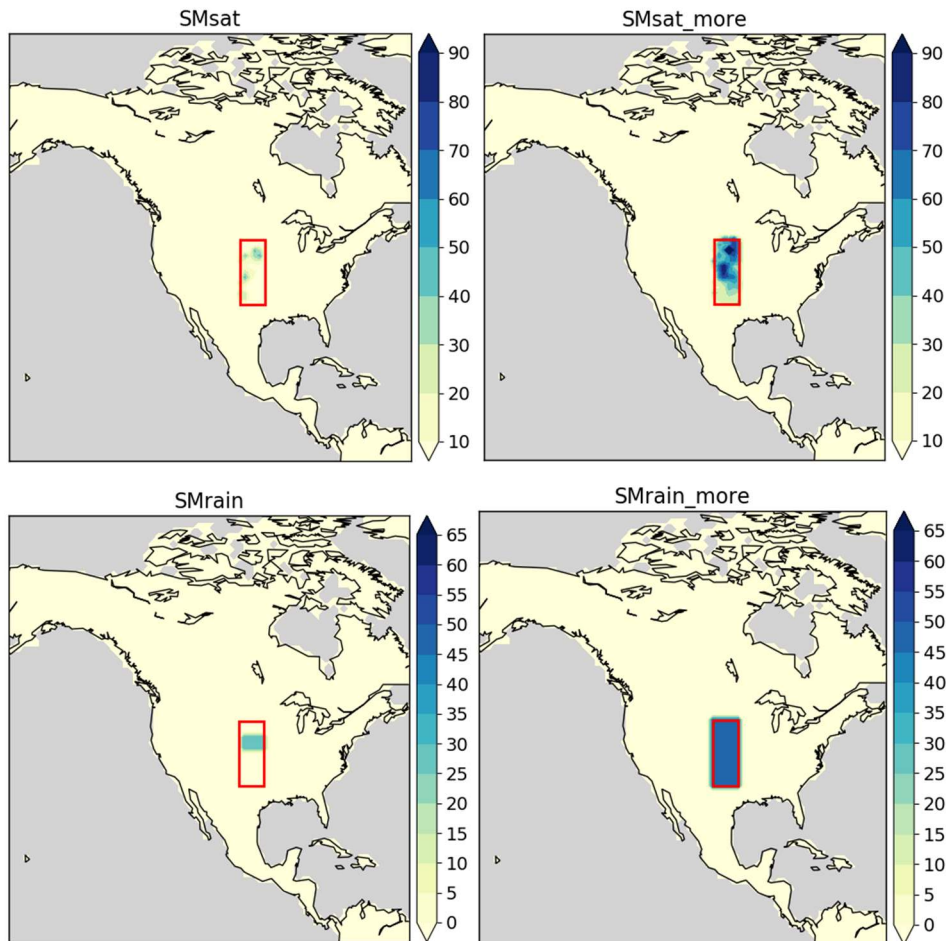


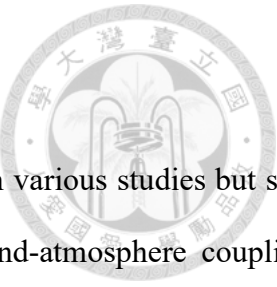
Figure 2-3 Irrigation rate (mm/month) for four irrigation experiments: (a) seasonal cycle averaged over 2001-2014, (b) spatial distribution of climatology JJA mean. The shading indicates the specified irrigated areas. The legend of (a) indicates the JJA climatology sum of each irrigation experiment.

Chapter 3 Results

3.1 Inference from GLACE Experiment

The term “land-atmosphere coupling” has been frequently appeared in various studies but still remains vague and ambiguous. We hope to explicate the concept of land-atmosphere coupling hotspots by reexamining the GLACE outputs. **Figure 3-1(a)** reproduces the distribution of hotspot regions shown in (Koster 2004; Koster et al. 2006) using the official Ω_p metric. The spatial pattern of coupling hotspot shows a close resemblance with Koster’s seminal work over central North America. We repeated the same process for evapotranspiration (ET) indicated as Ω_E in **Figure 3-1(b)**, and find the two metrics bear a striking resemblance in central North America, implying the signature of land-atmosphere coupling changes on the surface fluxes and/or a strong interconnection between the land and the atmosphere for local evapotranspiration to translate into precipitation. While it is natural to consider the local influence of soil moisture in the indicated hotspots, one should be noted that the indices refer to the general ability of soil moisture anomalies, either local or remote, to affect precipitation in a certain region.

As the spatial distribution of Ω_E reflects that central North America is also a hotspot region for the effect of land-atmosphere coupling on ET, we further examined the change in soil moisture-evapotranspiration (SM-ET) relationship between the LA-coupled and LA-uncoupled simulations. **Figure 3-2** shows that SM-ET relation is reduced in LA-uncoupled simulations. **Figure 3-3** reveals a regime shift in hydroclimates with and without land-atmosphere feedbacks. In LA-uncoupled simulations, the soil moisture is no longer the limiting factor for evapotranspiration, especially in wetter months such as June and July (**Figure 3-3a**). Given that the soil moisture values in LA-uncoupled simulations were overridden by the climatology of LA-coupled ones, the fact that the two sets of simulations have the same soil moisture climatology ascertains the higher capability of uncoupled runs to induce evapotranspiration. The same concept also applies within the LA-coupled simulations itself. **Figure 3-3(b)** shows the SM-ET relation of the ensemble mean from the LA-



coupled simulations. The dry-side soil moisture is located in the dry regime and contributes little to ET, while the wet-side soil moisture has already been saturated and the ET change cannot increase with higher soil moisture. In contrast, the soil moisture with moderate values lies within the transition zone and can contribute more ET than the total of both extremes (**Table 3-1**). **Figure 3-4** also shows that the small ET disappears in uncoupled runs, which might be an important cause of precipitation increase in uncoupled simulations.

3.2 Effect of Irrigation Prescriptions

To evaluate whether the change in soil moisture variability affects local precipitation, and whether the diverged irrigation response in modeling studies results from different irrigation prescriptions, we compared four irrigation experiments with two irrigation method with regard to their soil moisture variability and mean ET and precipitation changes. The difference in soil moisture, ET and precipitation for each irrigation experiment and GLACE is summarized in **Table 2-1**.

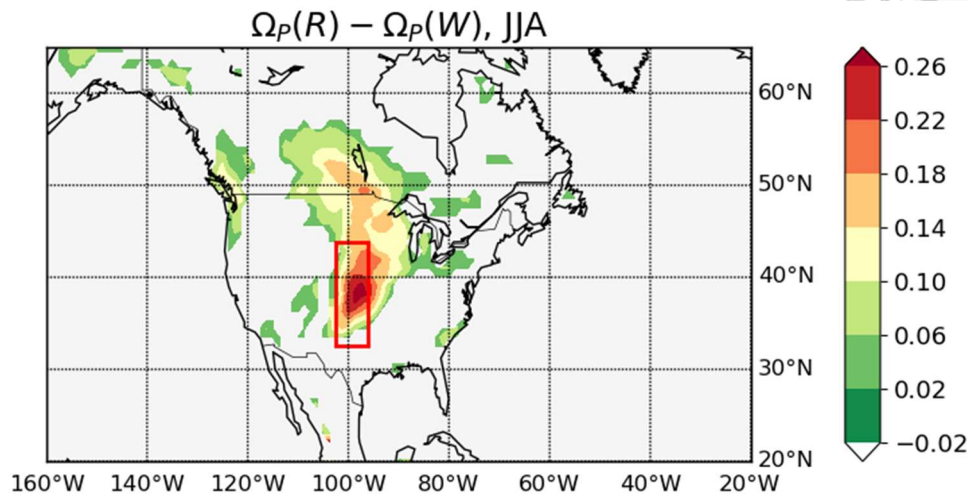
Figure 3-5 shows that flood irrigation (SMSat and SMSat_more) induces higher soil moisture values, whereas sprinkler irrigation (SMrain and SMrain_more) is more effective in enhancing ET, implying that the changes in ET is not purely determined by soil moisture variability as GLACE indicates. **Figure 3-6** displays the SM-ET relation for each irrigation experiment. Although most irrigation experiments are situated in the transitional or energy-limited regime, the ceiling of ET is slightly higher for sprinkler irrigation, leading to overall higher ET in sprinkler irrigation regardless of different irrigation water amounts. The higher limit in sprinkler irrigation might result from the rapid initial increase in near-surface water vapor in flood irrigation experiments, which reduces low-level water vapor deficit, thereby limiting the ET increase. Note that the hypothesis has not yet been confirmed and thereby requires more careful inspection.

On the other hand, even with a comparable ET increase to GLACE, the precipitation changes in the irrigation experiments are impartially limited and not as significant GLACE suggests (**Figure 3-5**). Notwithstanding, the soil moisture variability shows some footprints on both ET and

precipitation variability (**Figure 3-7**). The stronger the reduction of soil moisture variability, the stronger the reduction of ET and precipitation variability. The decreased interannual variability in precipitation can be interpreted as the dry years get wetter and the wetter years get drier. **Figure 3-8** shows the irrigation-induced changes for each year with regard to the precipitation in control simulation in each year. That the strong negative correlation only appears in flood irrigation experiments shows that the reduced precipitation variability coincides only with the reduced soil moisture variability but not mean increases in soil moisture values.

To further examine what caused GLACE to produce substantial precipitation increase in their uncoupled simulations, we plotted the vertical profile of divergence wind field for both GLACE and irrigation experiments (**Figure 3-9**). We find that the LA-coupled and LA-uncoupled simulations in GLACE both possess a strong low-level convergence that favors the accumulation of near-surface moisture, whereas the low-level divergence appears in every irrigation experiment including control run. The low-level divergence followed by irrigation-induced evaporative cooling makes the thermodynamic environment more unfavorable for convection to initiate and develop. Note that there is also a profound difference in JJA mean soil moisture between GLACE and CESM irrigation experiments (**Table 3-2**), which might contribute to their difference in precipitation response. Yet the disagreement in model settings such as yearly-varying SSTs with climatology SST and the use of different versions of the land model have been shown to be irrelevant to the soil moisture differences. The control simulations using CLM4.5 or AMIP configuration as GLACE have a similar climatology to our current irrigation experiments (not shown).

(a) Land-atmosphere coupling metric using Ω_P



(b) Land-atmosphere coupling metric using Ω_E

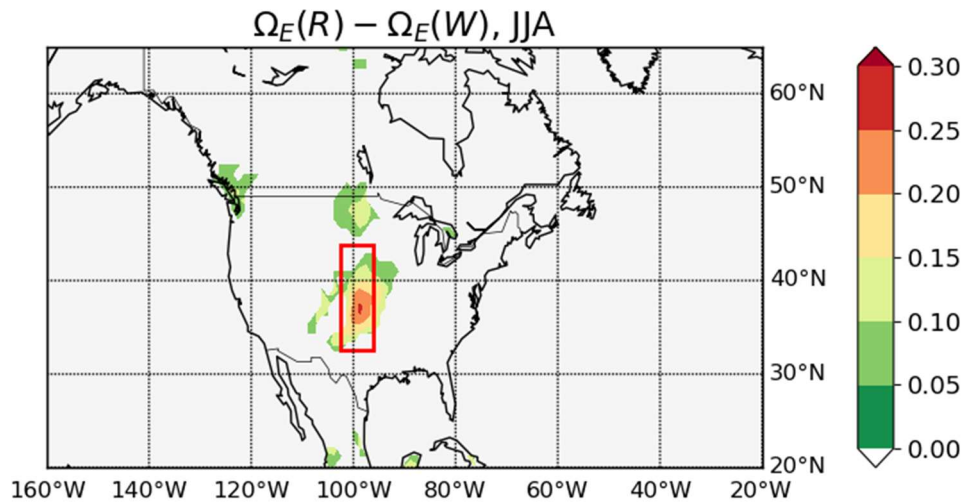


Figure 3-1 GLACE-style land-atmosphere coupling metric for (a) precipitation and (b) evapotranspiration (ET) variability in boreal summer (JJA) using 10 ensemble members over 1971-2014. The red box indicated the irrigated areas specified for the irrigation experiments. Note that the coupling hotspot distribution is sensitive to the timespan and the ensemble members chosen.

Change in SM-ET Relation in JJA

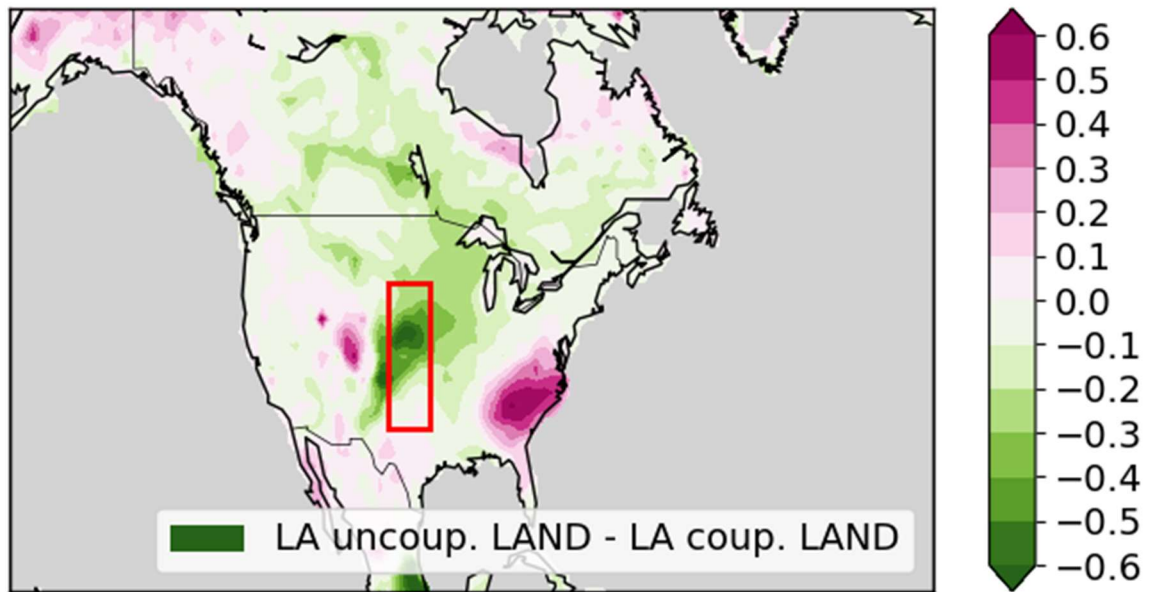


Figure 3-2 Effect of land-atmosphere coupling on soil moisture and evapotranspiration (SM-ET) correlations for ensemble mean in JJA from 1981-2014.

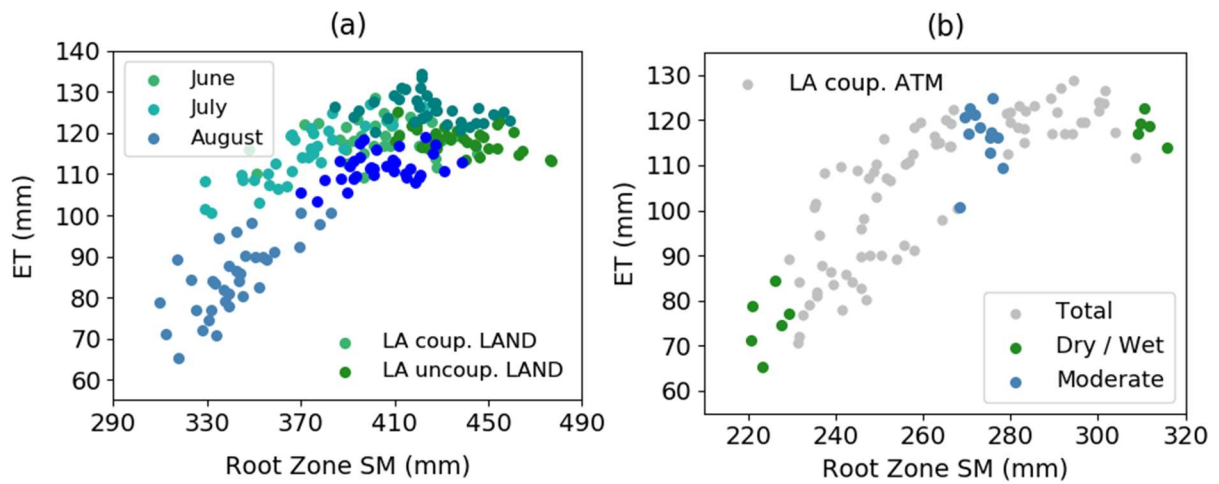


Figure 3-3 Effect of land-atmosphere coupling on SM-ET distribution for ensemble mean in JJA over the Great Plains (indicated in Figure 3-2), using (a) land-standalone (LAND) simulations, and (b) LA-coupled ATM simulations only. The darker dots of (a) indicate LA-uncoupled runs compared to LA-coupled runs. Gray dots in (b) shows the individual month of JJA for each year from 1981 to 2014. The green dots of (b) are the top and bottom 7% soil moisture in the probability distribution, which have equally the same average soil moisture values as the blue dots (see also Table 3-1).

Table 3-1 Comparison between JJA ET from dry- and wet-side soil moisture and ET from moderate soil moisture in LA-coupled ATM simulations averaged over the Great Plains. Units are mm/month.

Category	Moderate	Both-sides	Left 6% (Dry)	Right 6% (Wet)
Mean SM	247.23	247.25	209.38	285.12
Mean ET	103.84	91.59	67.72	115.46

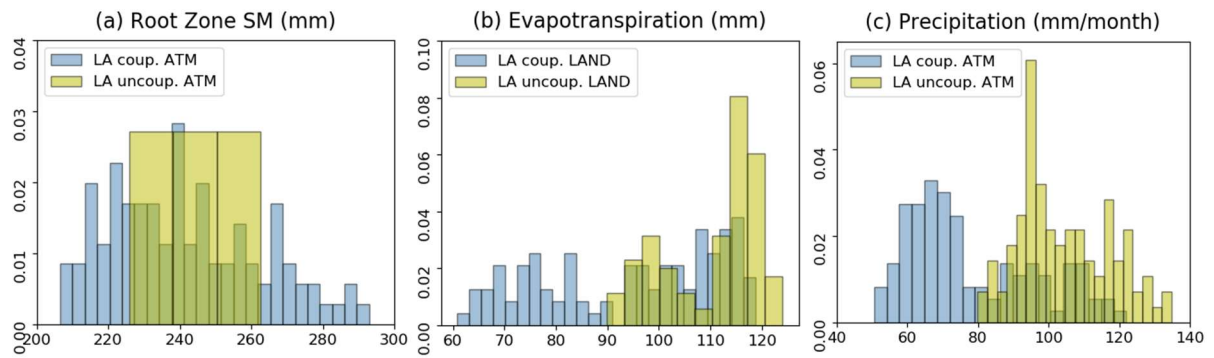


Figure 3-4 Effect of land-atmosphere coupling on distribution of monthly JJA (a) root zone soil moisture, (b) ET and (d) precipitation for the ensemble mean over the Great Plains. The y axis shows histogram densities. The legend indicates the coupled or uncoupled, land-atmosphere coupled or land-only set of simulations used for the corresponding variables. ATM simulations were used for atmospheric variables such as precipitation whereas LAND simulations for land surface variables such as soil moisture and ET. Here we present soil moisture distribution from ATM simulations to show the JJA soil moisture values from LA-uncoupled ATM were held fixed from the climatology of JJA LA-coupled ATM.

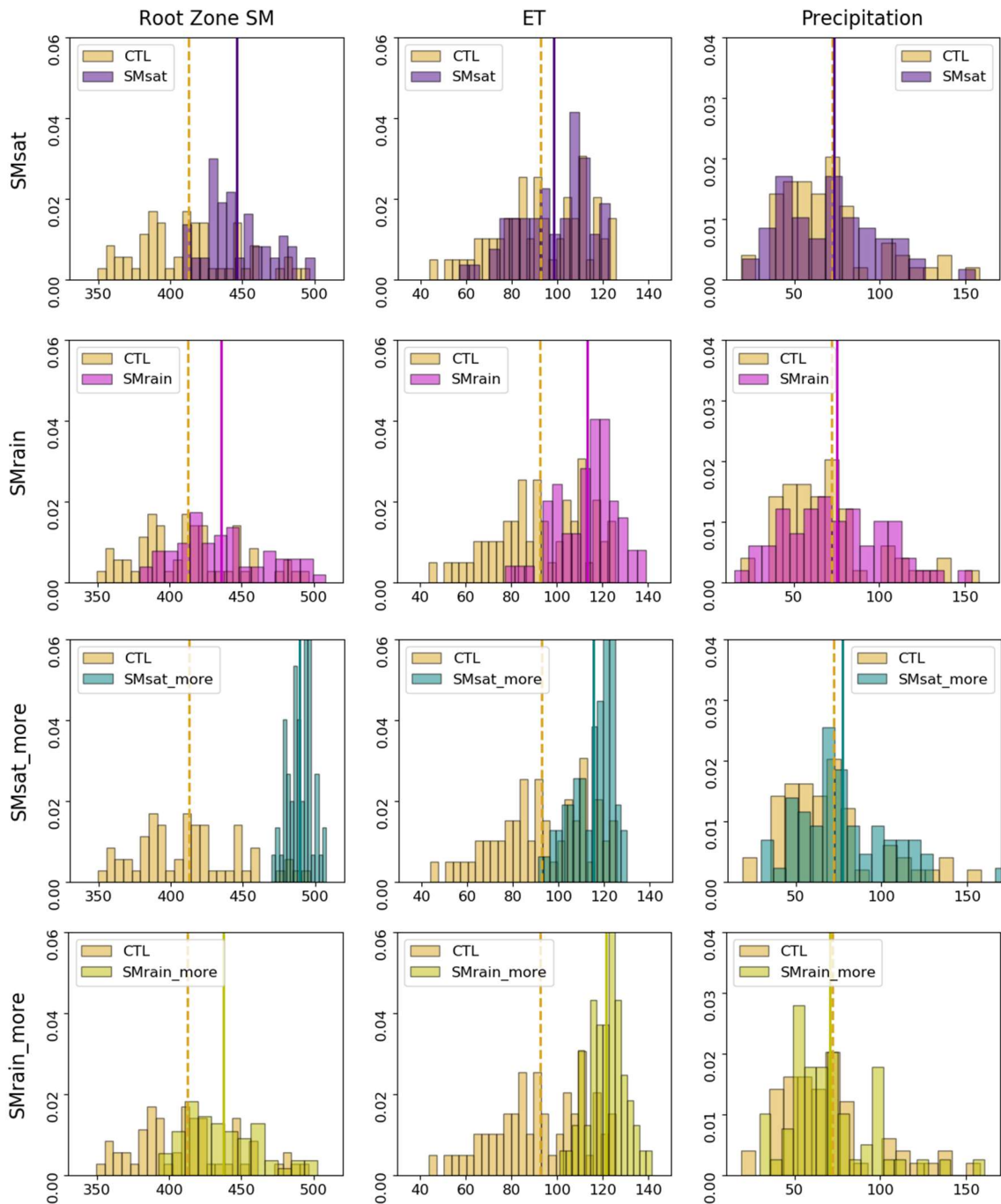


Figure 3-5 Effect of different irrigation prescriptions on distribution of monthly JJA root zone soil moisture, ET and precipitation in the Great Plains over the 20-year simulations: SMsat, SMrain, SMsat_more, SMrain_more. The y axis is histogram densities. The legend compares the control run with the irrigation run for each experiment. The vertical dashed line indicates the mean of control run, and the solid line indicates the mean of irrigation run. The units are mm/month.

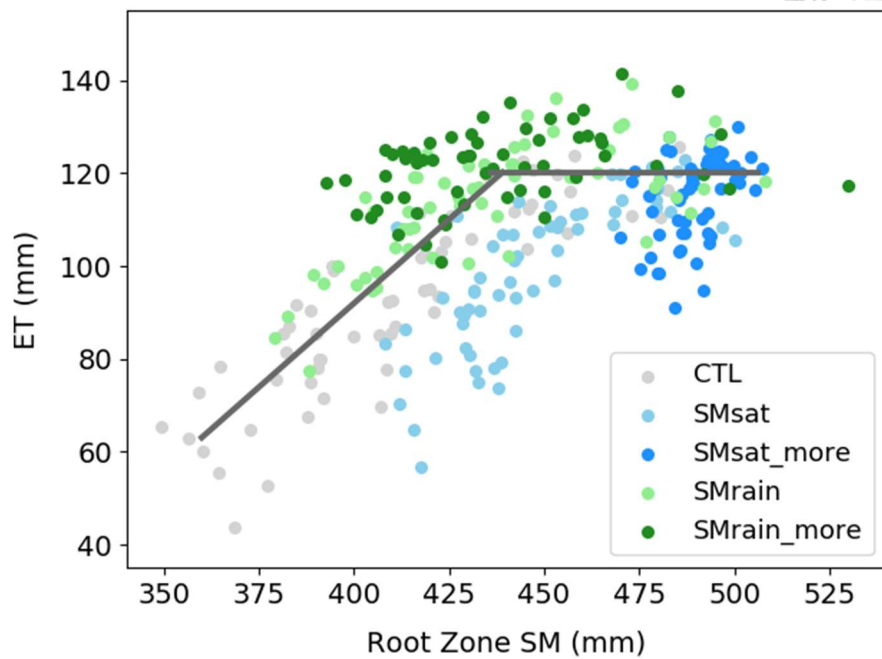


Figure 3-6 Effect of different irrigation prescriptions on SM-ET relationship using JJA monthly values over the 20-year simulations over the Great Plains. The blue dots indicate experiments using soil saturation (mimic flood irrigation) while the green dots indicate experiments using effective rain rate (mimic sprinkler irrigation). The gray line represents the Budyko curve and distinguishes the three hydrological regimes.

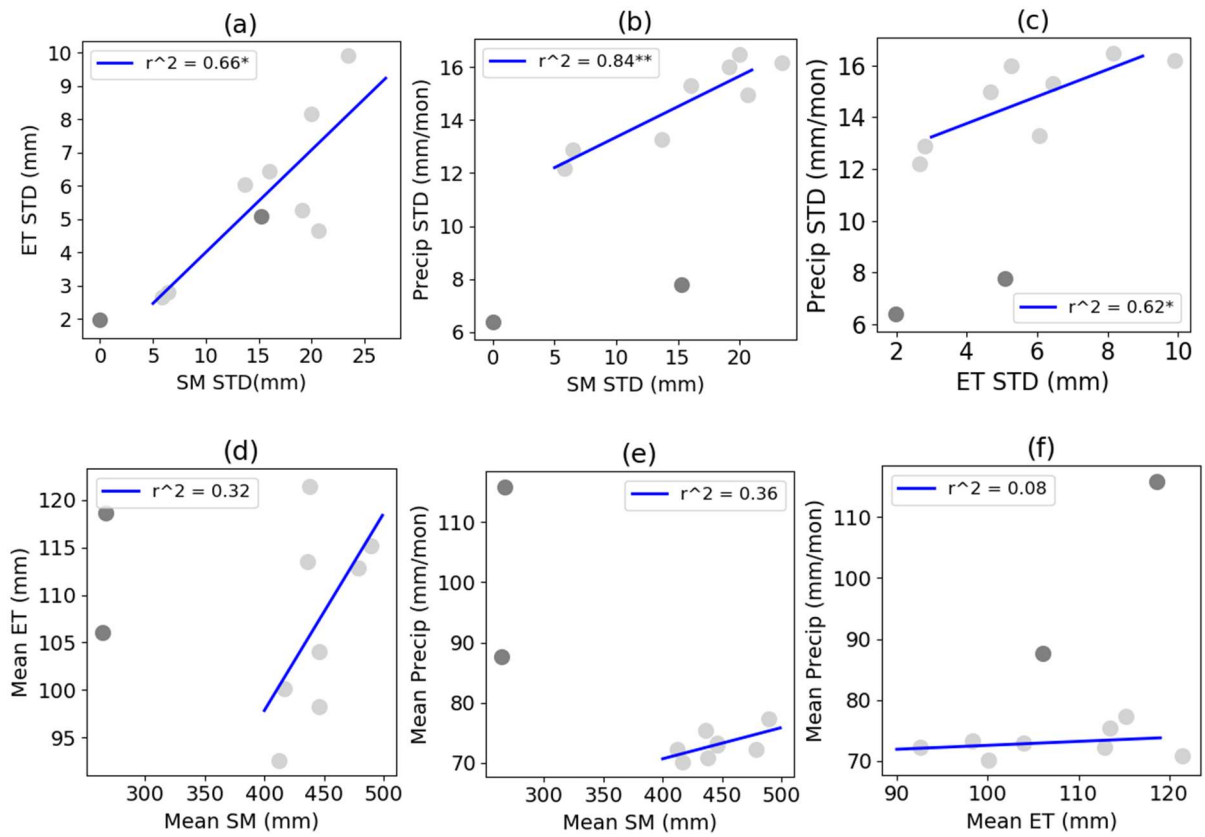


Figure 3-7 Distribution of SM-ET, SM-P and SM-ET for their JJA interannual standard deviation (a-c) and JJA climatology mean (d-f) over the Great Plains. The darker dots indicate data points from GLACE while the lighter dots indicate data points from irrigation experiments. The regression lines are computed only by data from irrigation experiments. * indicate significance level greater than 95% and ** indicate significance level greater than 99%.

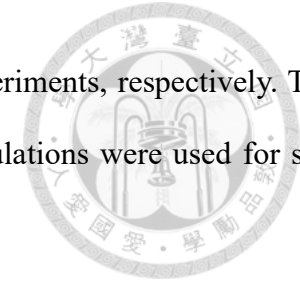


Table 3-2 Mean and standard deviation of JJA monthly soil moisture, ET and precipitation for GLACE and irrigation experiments, respectively. The standard deviation indicates interannual variability where JJA are averaged to remove intraseasonal variation. LAND simulations were used for soil moisture and ET in the GLACE experiment. The grids are averaged over the smaller box. Units: mm/month.

Casename	Top 1m Soil Moisture (mm)		ET (mm/mon)		Precipitation (mm/mon)	
	Mean	Standard deviation	Mean	Standard deviation	Mean	Standard deviation
LA-coupled	264.68	15.26	106.07	5.08	87.56	7.77
LA-uncoupled	267.22	5.68e-14	118.66	1.97	115.82	6.40
CTL	412.53	23.40	92.53	9.92	72.12	16.18
SMsat	445.90	13.69	98.31	6.05	73.21	13.27
SMsat_more	489.28	5.83	115.22	2.66	77.21	12.19
SMrain	435.93	19.14	113.50	5.26	75.31	16.00
SMrain_more	437.79	20.67	121.41	4.66	70.85	14.96

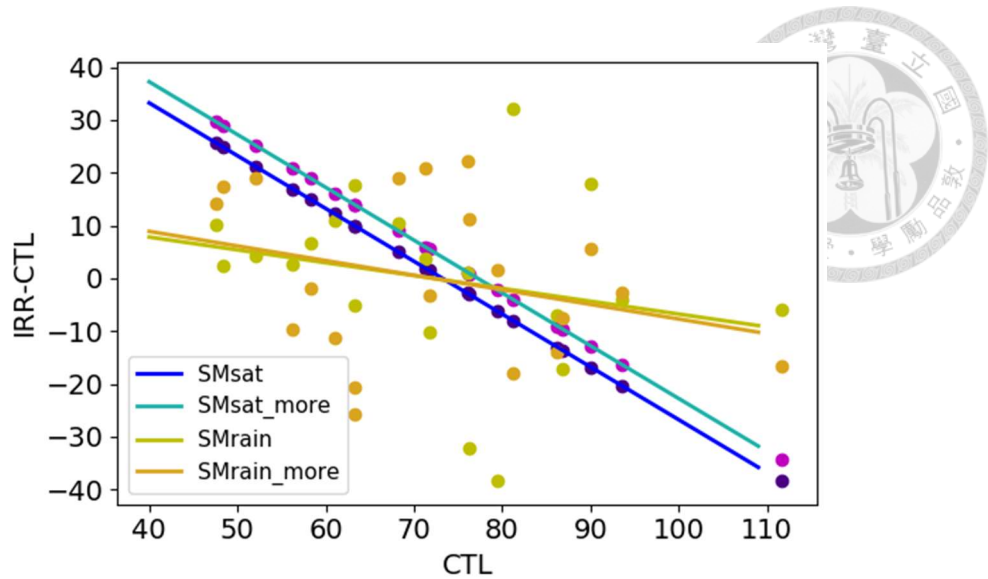


Figure 3-8 Interannual variation of irrigation-induced precipitation (mm/month) among the irrigation experiments over the Great Plains in JJA. The blue-tone dots are flood irrigation experiments, whereas the orange-tone dots are sprinkler irrigation experiments.

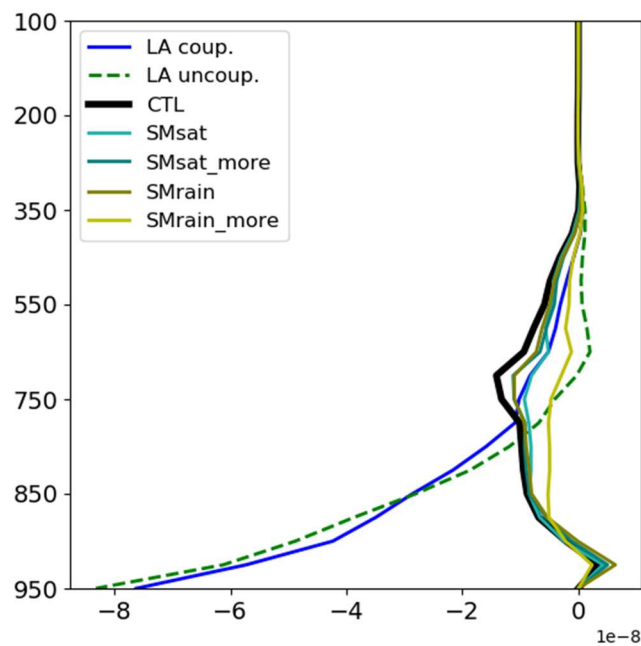
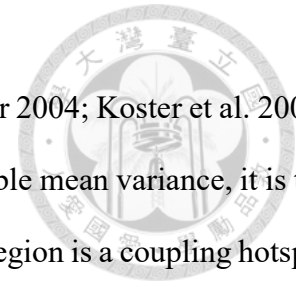


Figure 3-9 Vertical profile of divergence field over the Great Plains in JJA for each set of experiments. The blue solid line is the ensemble mean of LA-coupled simulations from GLACE, while the green dashed line is the ensemble mean of LA-uncoupled simulations. The remainder are from irrigation experiments.

Chapter 4 Summary and Discussion



Since the original land-atmosphere coupling index by GLACE (Koster 2004; Koster et al. 2006) is derived from the difference between intra-ensemble variance and ensemble mean variance, it is the variability driven by land-atmosphere coupling that determines whether a region is a coupling hotspot. By showing that different irrigation approaches also change the soil moisture variability, we partially reconcile the disparity among the modeling studies: for those who adopted surface irrigation (Harding and Snyder 2012) or directly prescribed ET rate (Segal et al. 1998) to guarantee sufficient moisture flux in the atmosphere, precipitation response can be significant. Conversely, for those who adopted sprinkler method in the model (Pei et al. 2016; Lu et al. 2017), insignificant or reduced rainfall is observed. Note that irrigated fraction also matters, and is probably more important than soil moisture variability changes. For instance, the difference between SMSat and SMSat_more is that the latter irrigated for the entire C3 crop whereas the former only irrigated for around half of the C3 crop fraction, which leads to significant differences in both ET and precipitation response. This might explain why Adegoke et al. (2003) irrigated by saturating the soil columns once per day but obtained insignificant precipitation changes. Contrarily, while Puma and Cook (2010) chose to irrigate by adding water to the topsoil, their choice to irrigate for the entire vegetated fraction is likely at play in determining the significant irrigation signal.

We also show that the precipitation variability is more susceptible to change when soil moisture variability changes, which explains why central North America is identified as a coupling hotspot. As coupling hotspots are originally defined as the locations that are more capable to improve seasonal forecasts, variability matters more than mean changes because a robust response with little variation is hard to provide a strong signal for longer-term forecasts. For instance, even if the evaporation response to soil moisture is robust, the atmosphere is unlikely to show a strong signal at the surface when the evaporation variability is low. The reduced precipitation variability followed by reduced soil moisture variability suggests a negative feedback from the soil moisture to the precipitation. That

is, irrigation tends to mediate precipitation by decreasing rainfall in wet years and increasing in dry years (**Figure 3-8**). While this finding is contradictory to a handful of studies suggesting that irrigation tends to amplify precipitation but may not be able to trigger convection (Schickedanz 1976; Segal et al. 1998; Harding and Snyder 2012; Huber et al. 2014; Welty and Zeng 2018), we further examined the divergence field with interannual variation. **Figure 4-1** shows the divergence changes in dry years and wet years. The wet (dry) years is determined by whether the mean JJA precipitation of that year is higher (lower) than the average of the 20-year simulations. The results show that irrigation tends to induce low-level divergence in dry years and low-level convergence in wet years, whereas wet years have stronger low-level divergence than dry years (the gray lines in **Figure 4-1**). The relation between moisture divergence and precipitation remains obscure, while the irrigation effect on precipitation on interannual scale in this study requires more vigorous evidence.

Table 4-1 further divides the variance of precipitation into three components: the variance of ET, the variance of vertically-integrated divergence and the covariance between ET and divergence. Assume precipitation can be separated into the contribution of ET and divergence, then

$$\text{var}(P) = \text{var}(ET) + \text{var}(D) + 2 \text{cov}(ET, D) \quad (4.1)$$

Note that we computed the divergence using the concept of moisture budget conservation, i.e. $D' = P' - ET' - \frac{dQ}{dt}$, where D' denotes the anomaly of divergence, P' denotes the precipitation anomaly, ET' denotes the evapotranspiration anomaly, and $\frac{dQ}{dt}$ denotes the rate of change in humidity. We chose this approach because we do not have outputs for each timestep. In addition, the divergence term calculated by monthly outputs would not be conserved over lands, since the monthly wind fields have smoothed out the transient variation. **Table 4-1** shows that the reduced variance in P after irrigation is primarily contributed by the changes in ET variance and covariance term despite the marked increase in divergence variance. Since the covariance term is purely a mathematical outcome and might not correspond to certain physical processes, we treat it as a nonlinear term in this variance analysis. While the changes in ET may represent the changes in local moisture sources, the changes

in divergence can indicate the changes in outer moisture sources. The dominant role of ET changes in reducing P variability suggests that the local moisture contribution is more important over this region. **Table 4-2** further shows the coefficient of determination (R^2) of the P-ET and P-D relationship using a simple linear regression model. Since R^2 can be regarded as the proportion of P variance explained by ET or divergence, the weak P-ET relationship in SMSat, for example, indicates the strong contribution of ET on the significant reduction in P variability.

When it comes to the inconsistent or insignificant irrigation impacts over the Great Plains, a recent study (Tuttle and Salvucci 2016) used Granger causality to estimate the relationship between soil moisture and subsequent precipitation across the United States, and suggested that ET may not strongly influence precipitation in this region. Given that much of the precipitation over the Great Plains occurs nocturnally because of eastward-propagating convective systems originating in the upstream of the irrigated areas, it is likely that local land-atmosphere interactions are not important, at least not dominant, for predicting rainfall in this region. The propagation of the mesoscale convective systems (MCS) from Rocky Mountains can thus provide a favorable environment for the enhanced moisture from irrigation to take effect. Although our irrigation experiments also show a nighttime rainfall increase from irrigation (**Figure 4-2**), the model nocturnal rainfall is much less than the afternoon rainfall in terms of total rainfall, making the irrigation-induced changes comparatively negligible. Similarly, Pan et al. (1996) stressed the importance of sensible heating in the convective initiation and showed that the increase in soil moisture can decrease local rainfall when the atmosphere was humid and lack sufficient thermal forcing to initiate convection. The general increasing trend suggested by observational studies might therefore be associated with large-scale oceanic forcings. For instance, Hu et al. (2011) revealed that Atlantic multidecadal oscillation (AMO) provides a fundamental control on JJA precipitation over North America, especially during the cold phase, which incidentally matches the period of irrigation expansion and might overshadow the irrigation effect.

It is worth noting that the empirical relationship between predictors of land and atmosphere is

not linear and may subject to change over time, for instance, due to climate change (Seneviratne et al. 2013) and/or land use and land cover change (LULCC, Hirsch et al. 2014; McDermid et al. 2019). The potential implication is twofold: (1) one may not expect the precipitation response to be proportional to the land surface changes, for the relationship is nonstationary; (2) it is probable that the coupling hotspot regions identified by GLACE is not always valid, and that irrigation might weaken the coupling hotspot over the Great Plains (Lu et al. 2017). However, one cannot separate the irrigation effect on land-atmosphere coupling strength and the outcome of land-atmosphere interactions such as precipitation, which is why we do not prefer to apply the postulate of “irrigation weakens the coupling strengths” to explain the insignificant precipitation changes, and the other way around (Lu et al. 2017; McDermid et al. 2019). It is also not justifiable to say irrigation cannot take effect over the Great Plains because the surface cooling surpasses the surface moistening, as the irrigation-induced cooling can also act as the cold pool for the MCS to develop. The increased stability of the atmosphere caused by surface cooling also might not be as dominant as the low-level divergence while the latter does not always occur in irrigation scenarios. One should be mindful when interpreting the mutual-causal relationship.

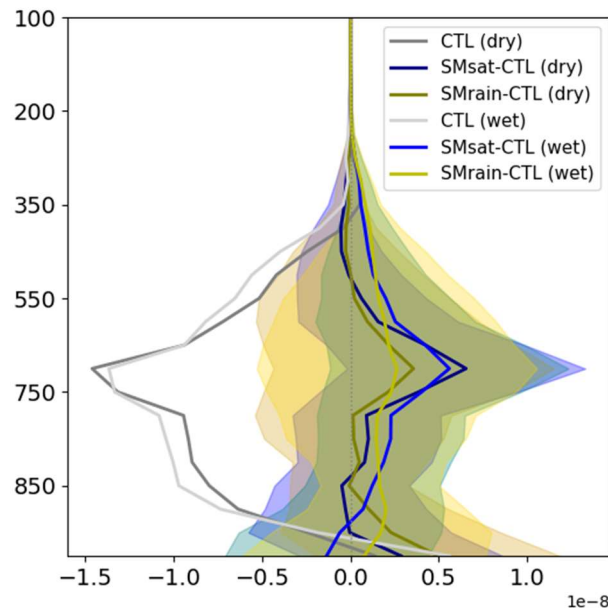
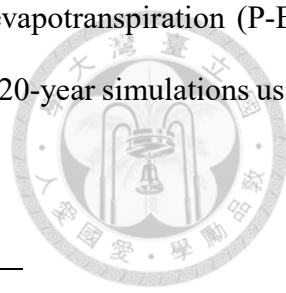


Figure 4-1 Vertical profile of divergence field over the Great Plains in JJA for two irrigation prescriptions in dry and wet years. The darker lines indicate the dry years while lighter lines are the wet years. The blue (orange)-tone lines are flood (sprinkler) irrigation experiments. The gray lines indicate control runs.

Table 4-1 Variance decomposition of mean JJA precipitation for each year averaged over the Great Plains for the irrigation experiments. P indicates precipitation, and D indicates vertical-integrated divergence. The units for the variance are mm^2 .

	Var (P)	Var (ET) + Var (D) + 2*Cov (ET,D)	Var (ET)	Var (Q)	Var (D)	2*Cov (ET, D)
CTL	261.82	262.52	98.33	0.04	73.01	91.18
SMsat	176	143.4	7.08	0.54	146.58	-10.26
SMsat_more	148.48	165.39	36.63	0.69	90.96	37.8
SMrain	255.9	255.78	27.7	0.08	187.62	40.46
SMrain_more	223.94	209.98	21.72	1.05	153.06	35.2

Table 4-2 Coefficient of determination (R^2) for JJA mean precipitation-evapotranspiration (P-ET) and precipitation-divergence (P-D) relationship in the Great Plains over the 20-year simulations using the simple linear regression model.



R^2	P-ET	P-D
CTL	0.79	0.72
SMsat	0.005	0.95
SMsat_more	0.53	0.77
SMrain	0.32	0.89
SMrain_more	0.35	0.89

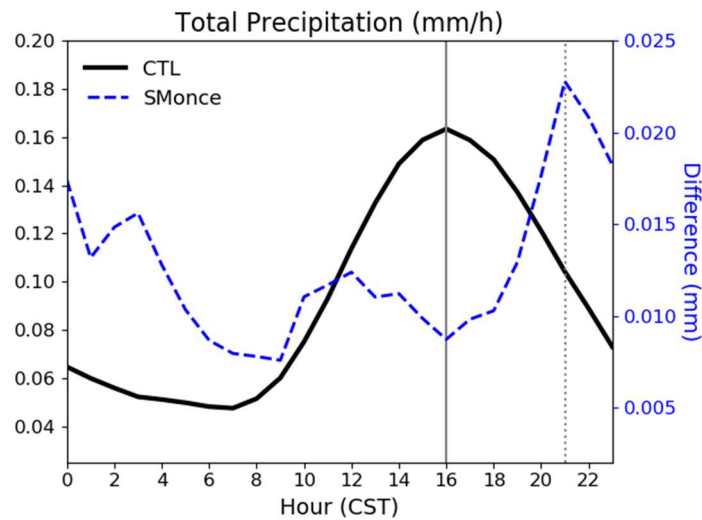
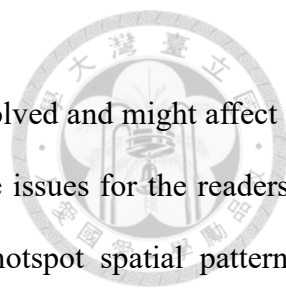


Figure 4-2 Diurnal cycle of total precipitation over the Great Plains for control simulations and irrigation runs in unit of mm/hr. The black solid line indicates control run while the blue dashed shows the irrigation-induced rainfall changes. SMonce is similar to SMsat with the top1m soil moisture set to field capacity once per day.

Chapter 5 Future work



In our preliminary analysis, some important issues have not been resolved and might affect the credibility of our results. The author feels it is necessary to address these issues for the readers to interpret these data. First and foremost, we found that the coupling hotspot spatial pattern is susceptible to change when we considered fewer ensemble members and simulation years. Since we can only obtain 9 ensemble members for the LAND simulations, we also computed the coupling hotspot indices using the corresponding 9 ensemble members in ATM simulations, causing the coupling hotspot over central North America to disappear. In addition, to compare with the irrigation experiments, we also have considered using the same length of the years for analysis, but the 20-year simulations from GLACE cannot reproduce a similar spatial pattern of coupling strengths shown in the literature. Secondly, the results of our irrigation experiments are also sensitive to the choice of timespan and areal size for spatial averaging. Since we only have 25-year (and a few 30-year) simulations for each experiment, we initially considered removing the first 10 years as a spin-up period and analyzed the last 20 years for the simulations having 30-year long. We eventually removed the first 5 years to incorporate more experiments, and found that the same 20-year (year 6 to year 25 vs. year 11 to year 30) shows a stark difference in precipitation variability: the stronger reduction in precipitation variability in flood irrigation experiment no longer exists. In addition, since the irrigated areas are not of the equal size for the four selected irrigation experiments, we chose to perform the areal mean using the smaller grid box. However, after we corrected the irrigated areas in SMrain to be consistent with others, the irrigation response in ET and precipitation behaves much differently (**Table 5-1**, **Table 5-2**), making the aforementioned conclusions not hold anymore. As we cannot be sure whether the problem results from this irrigation run or the areal size for averaging, we did not show the outcomes using this version of SMrain.

We also found the conventional 10-year spin-up period for land-atmosphere coupled runs might be insufficient for central North America, where the groundwater table depth has not reached a steady

state in the 30-year cold-start control simulations (**Figure 5-1**). This dry bias in soil moisture and hydrology is likely to affect the results, as previous studies have shown a higher land-driven predictability and land-atmosphere coupling over North America during wet years (Schubert et al. 2008; Guo and Dirmeyer 2013; Kumar et al. 2014). However, this does not mean the above results are untenable, as land-atmosphere coupled simulations in general can reach equilibrium in one year. In addition, since the average groundwater table depth is about 5-10 meters deep, the top 1m soil moisture should not be drastically different if using longer simulations. On the other hand, as Ho (2017) indicated the potential impact of irrigated area size on the atmospheric response, our irrigation experiments were performed under a medium size of irrigated areas, which can show little changes in precipitation in their sensitivity tests. Current experiments can be amended using larger irrigated areas as Ho (2017) indicated to address the relative importance of irrigated areas, soil moisture variability and soil moisture mean changes. However, we do not expect a drastic increase in precipitation even using larger irrigated areas. The magnitude of precipitation increase in larger irrigated areas is also much weaker than the decrease in smaller irrigated areas in Ho (2017).

A few interesting topics associated with GLACE and irrigation are also worth exploring. While GLACE suggested that land-atmosphere coupling can enhance subseasonal-to-seasonal predictability, the impact of irrigation on potential land-driven predictability has not been well established. The analogy between irrigation and decoupled land-atmosphere feedbacks is also elusive. Current results also do not show consistent signs in changes of precipitation mean and variability for land-atmosphere coupling hotspots, but the implication and physical mechanism have not been unveiled either. In addition, while previous findings suggested that irrigation can only amplify precipitation (Schickedanz 1976; Segal et al. 1998; Harding and Snyder 2012; Huber et al. 2014), some studies such as D'Odorico and Porporato (2004) indicated a positive soil moisture-precipitation feedback through rainfall-triggering mechanisms. Whether the difference comes from the nature of simple soil wetting and irrigation or spatial disparity between the state of Illinois and the Great Plains can be explored to have deeper understanding of the nature of irrigation processes.

Table 5-1 Same as Table 3-2, but included another SMrain experiment which irrigated over a larger extent (denoted as SMrain’).

Casename	Top 1m Soil Moisture (mm)		ET (mm/mon)		Precipitation (mm/mon)	
	Mean	Standard deviation	Mean	Standard deviation	Mean	Standard deviation
LA-coupled	264.68	15.26	106.07	5.08	87.56	7.77
LA-uncoupled	267.22	5.68e-14	118.66	1.97	115.82	6.40
CTL	412.53	23.40	92.53	9.92	72.12	16.18
SMSat	445.90	13.69	98.31	6.05	73.21	13.27
SMSat_more	489.28	5.83	115.22	2.66	77.21	12.19
SMrain	435.93	19.14	113.50	5.26	75.31	16.00
SMrain’	431.23	16.91	104.47	8.18	80.96	10.39
SMrain_more	437.79	20.67	121.41	4.66	70.85	14.96

Table 5-2 Similar to Table 5-1, but the grids were averaged over the large box (red box indicated in Figure 2-1).

Casename	Top 1m Soil Moisture (mm)		ET (mm/mon)		Precipitation (mm/mon)	
	Mean	Standard deviation	Mean	Standard deviation	Mean	Standard deviation
LA-coupled	254.76	13.22	104.69	4.07	88.72	6.94
LA-uncoupled	256.78	5.68e-14	116.11	1.88	115.53	5.44
CTL	394.79	20.03	90.46	9.27	74.22	15.39
SMSat	418.01	12.70	93.85	5.87	74.40	11.98
SMSat_more	458.10	5.29	110.06	2.45	79.25	10.61
SMrain	407.35	16.30	100.37	6.10	75.96	13.35
SMrain’	410.46	14.83	101.57	7.43	81.81	10.46
SMrain_more	419.09	17.98	119.19	4.16	74.86	12.20

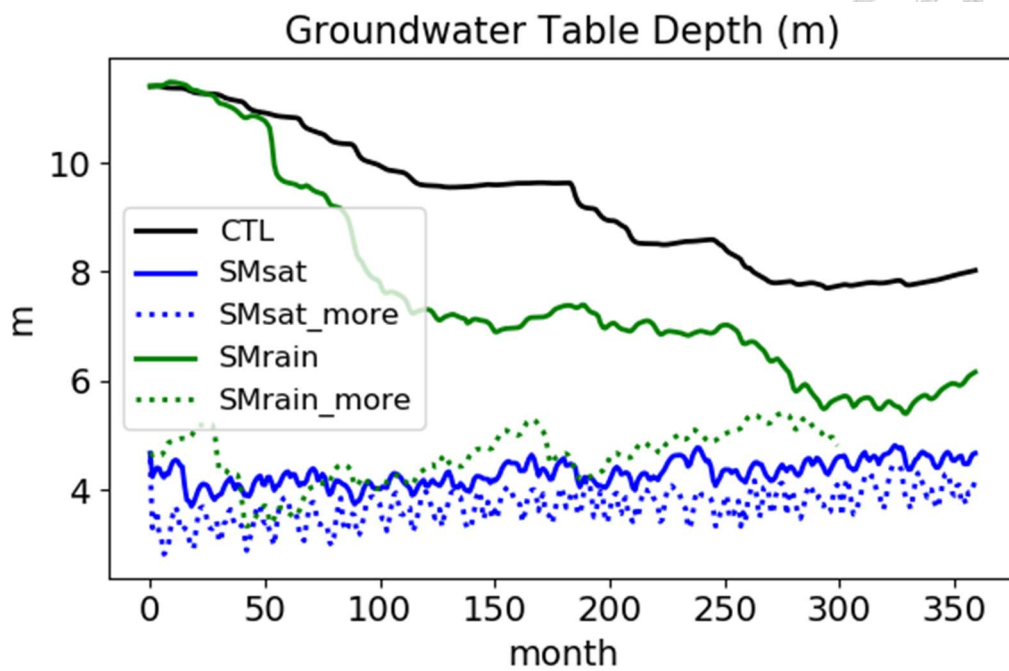
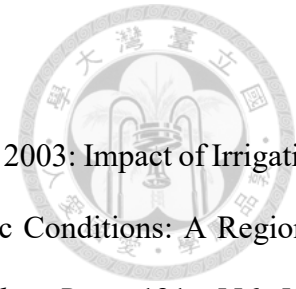


Figure 5-1 Variation of groundwater table depth over time for the irrigation experiments in the Great Plains over the course of simulation years.

REFERENCES



- Adegoke, J. O., R. A. Pielke, J. Eastman, R. Mahmood, and K. G. Hubbard, 2003: Impact of Irrigation on Midsummer Surface Fluxes and Temperature under Dry Synoptic Conditions: A Regional Atmospheric Model Study of the U.S. High Plains. *Mon. Weather Rev.*, **131**, 556–564, [https://doi.org/10.1175/1520-0493\(2003\)131<0556:IOIOMS>2.0.CO;2](https://doi.org/10.1175/1520-0493(2003)131<0556:IOIOMS>2.0.CO;2).
- Alter, R. E., Y. Fan, B. R. Lintner, and C. P. Weaver, 2015a: Observational Evidence that Great Plains Irrigation Has Enhanced Summer Precipitation Intensity and Totals in the Midwestern United States. *J. Hydrometeorol.*, **16**, 1717–1735, <https://doi.org/10.1175/JHM-D-14-0115.1>.
- , E.-S. Im, and E. A. B. Eltahir, 2015b: Rainfall consistently enhanced around the Gezira Scheme in East Africa due to irrigation. *Nat. Geosci.*, **8**, 763–767, <https://doi.org/10.1038/ngeo2514>.
- Barnston, A. G., and P. T. Schickedanz, 1984: The Effect of Irrigation on Warm Season Precipitation in the Southern Great Plains. *J. Clim. Appl. Meteorol.*, **23**, 865–888, [https://doi.org/10.1175/1520-0450\(1984\)023<0865:TEOIOW>2.0.CO;2](https://doi.org/10.1175/1520-0450(1984)023<0865:TEOIOW>2.0.CO;2).
- van Bavel, C. H. M., F. S. Nakayama, and W. L. Ehrlter, 1965: Measuring Transpiration Resistance of Leaves. *Plant Physiol.*, **40**, 535–540, <https://doi.org/10.1104/pp.40.3.535>.
- Berg, A., B. R. Lintner, K. L. Findell, S. Malyshev, P. C. Loikith, and P. Gentine, 2014: Impact of Soil Moisture–Atmosphere Interactions on Surface Temperature Distribution. *J. Clim.*, **27**, 7976–7993, <https://doi.org/10.1175/JCLI-D-13-00591.1>.
- Budyko, M. I., 1956: *Тепловой баланс земной поверхности (Heat Balance of the Earth's Surface)*. Gidrometeoizdat, Leningrad, 255pp.
- , 1974: *Climate and Life*. Academic Press, Inc., 508pp.
- Ceglar, A., A. Toreti, C. Prodhomme, M. Zampieri, M. Turco, and F. J. Doblas-Reyes, 2018: Land-surface initialisation improves seasonal climate prediction skill for maize yield forecast. *Sci. Rep.*, **8**, 1322, <https://doi.org/10.1038/s41598-018-19586-6>.
- Cook, B. I., M. J. Puma, and N. Y. Krakauer, 2011: Irrigation induced surface cooling in the context

of modern and increased greenhouse gas forcing. *Clim. Dyn.*, **37**, 1587–1600, <https://doi.org/10.1007/s00382-010-0932-x>.

D’Odorico, P., and A. Porporato, 2004: Preferential states in soil moisture and climate dynamics. *Proc. Natl. Acad. Sci.*, **101**, 8848–8851, <https://doi.org/10.1073/pnas.0401428101>.

DeAngelis, A., F. Dominguez, Y. Fan, A. Robock, M. D. Kustu, and D. Robinson, 2010: Evidence of enhanced precipitation due to irrigation over the Great Plains of the United States. *J. Geophys. Res.*, **115**, D15115, <https://doi.org/10.1029/2010JD013892>.

Dirmeyer, P. A., 2003: The Role of the Land Surface Background State in Climate Predictability. *J. Hydrometeorol.*, **4**, 599–610, [https://doi.org/10.1175/1525-7541\(2003\)004<0599:TROTLS>2.0.CO;2](https://doi.org/10.1175/1525-7541(2003)004<0599:TROTLS>2.0.CO;2).

———, and Coauthors, 2012: Evidence for Enhanced Land–Atmosphere Feedback in a Warming Climate. *J. Hydrometeorol.*, **13**, 981–995, <https://doi.org/10.1175/JHM-D-11-0104.1>.

———, S. Kumar, M. J. Fennessy, E. L. Altshuler, T. DelSole, Z. Guo, B. A. Cash, and D. Straus, 2013: Model Estimates of Land-Driven Predictability in a Changing Climate from CCSM4. *J. Clim.*, **26**, 8495–8512, <https://doi.org/10.1175/JCLI-D-13-00029.1>.

———, Z. Wang, M. J. Mbuh, and H. E. Norton, 2014: Intensified land surface control on boundary layer growth in a changing climate. *Geophys. Res. Lett.*, **41**, 1290–1294, <https://doi.org/10.1002/2013GL058826>.

Douville, H., 2010: Relative contribution of soil moisture and snow mass to seasonal climate predictability: a pilot study. *Clim. Dyn.*, **34**, 797–818, <https://doi.org/10.1007/s00382-008-0508-1>.

Fan, J., B. McConkey, H. Wang, and H. Janzen, 2016: Root distribution by depth for temperate agricultural crops. *F. Crop. Res.*, **189**, 68–74, <https://doi.org/10.1016/j.fcr.2016.02.013>.

Findell, K. L., P. W. Keys, R. J. van der Ent, B. R. Lintner, A. Berg, and J. P. Krasting, 2019: Rising Temperatures Increase Importance of Oceanic Evaporation as a Source for Continental Precipitation. *J. Clim.*, **32**, 7713–7726, <https://doi.org/10.1175/JCLI-D-19-0145.1>.

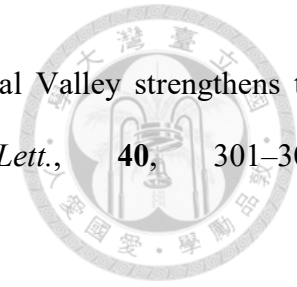
- Gates, W. L., 1992: AMIP: The Atmospheric Model Intercomparison Project. *Bull. Am. Meteorol. Soc.*, **73**, 1962–1970, [https://doi.org/10.1175/1520-0477\(1992\)073<1962:ATAMIP>2.0.CO;2](https://doi.org/10.1175/1520-0477(1992)073<1962:ATAMIP>2.0.CO;2).
- Guo, Z., and P. A. Dirmeyer, 2013: Interannual Variability of Land–Atmosphere Coupling Strength. *J. Hydrometeorol.*, **14**, 1636–1646, <https://doi.org/10.1175/JHM-D-12-0171.1>.
- , and Coauthors, 2006: GLACE: The Global Land–Atmosphere Coupling Experiment. Part II: Analysis. *J. Hydrometeorol.*, **7**, 611–625, <https://doi.org/10.1175/JHM511.1>.
- , P. A. Dirmeyer, and T. DelSole, 2011: Land surface impacts on subseasonal and seasonal predictability. *Geophys. Res. Lett.*, **38**, n/a-n/a, <https://doi.org/10.1029/2011GL049945>.
- Halder, S., P. A. Dirmeyer, L. Marx, and J. L. Kinter, 2018: Impact of Land Surface Initialization and Land-Atmosphere Coupling on the Prediction of the Indian Summer Monsoon with the CFSv2. *Front. Environ. Sci.*, **5**, 92, <https://doi.org/10.3389/fenvs.2017.00092>.
- Harding, K. J., and P. K. Snyder, 2012: Modeling the Atmospheric Response to Irrigation in the Great Plains. Part I: General Impacts on Precipitation and the Energy Budget. *J. Hydrometeorol.*, **13**, 1667–1686, <https://doi.org/10.1175/JHM-D-11-098.1>.
- Hirsch, A. L., J. Kala, A. J. Pitman, C. Carouge, J. P. Evans, V. Haverd, and D. Mocko, 2014: Impact of Land Surface Initialization Approach on Subseasonal Forecast Skill: A Regional Analysis in the Southern Hemisphere. *J. Hydrometeorol.*, **15**, 300–319, <https://doi.org/10.1175/JHM-D-13-05.1>.
- Ho, A.-C., 2017: Responses of Land-Atmosphere Interactions to the Change in Irrigation Area Size. *M. S. thesis, Natl. Taiwan Univ.*, <https://doi.org/10.6342/NTU201701733>.
- Hu, Q., S. Feng, and R. J. Oglesby, 2011: Variations in North American Summer Precipitation Driven by the Atlantic Multidecadal Oscillation. *J. Clim.*, **24**, 5555–5570, <https://doi.org/10.1175/2011JCLI4060.1>.
- Huber, D., D. Mechem, and N. Brunzell, 2014: The Effects of Great Plains Irrigation on the Surface Energy Balance, Regional Circulation, and Precipitation. *Climate*, **2**, 103–128, <https://doi.org/10.3390/cli2020103>.

- Hurrell, J. W., J. J. Hack, D. Shea, J. M. Caron, and J. Rosinski, 2008: A New Sea Surface Temperature and Sea Ice Boundary Dataset for the Community Atmosphere Model. *J. Clim.*, **21**, 5145–5153, <https://doi.org/10.1175/2008JCLI2292.1>.
- , and Coauthors, 2013: The Community Earth System Model: A Framework for Collaborative Research. *Bull. Am. Meteorol. Soc.*, **94**, 1339–1360, <https://doi.org/10.1175/BAMS-D-12-00121.1>.
- Im, E.-S., M. P. Marcella, and E. A. B. Eltahir, 2014: Impact of Potential Large-Scale Irrigation on the West African Monsoon and Its Dependence on Location of Irrigated Area. *J. Clim.*, **27**, 994–1009, <https://doi.org/10.1175/JCLI-D-13-00290.1>.
- Kim, Y., and G. Wang, 2012: Soil moisture-vegetation-precipitation feedback over North America: Its sensitivity to soil moisture climatology. *J. Geophys. Res. Atmos.*, **117**, 17584, <https://doi.org/10.1029/2012JD017584>.
- Koster, R. D., 2004: Regions of Strong Coupling Between Soil Moisture and Precipitation. *Science (80-.)*, **305**, 1138–1140, <https://doi.org/10.1126/science.1100217>.
- , and G. K. Walker, 2015: Interactive Vegetation Phenology, Soil Moisture, and Monthly Temperature Forecasts. *J. Hydrometeorol.*, **16**, 1456–1465, <https://doi.org/10.1175/JHM-D-14-0205.1>.
- Koster, R. D., M. J. Suarez, and M. Heiser, 2000: Variance and Predictability of Precipitation at Seasonal-to-Interannual Timescales. *J. Hydrometeorol.*, **1**, 26–46, [https://doi.org/10.1175/1525-7541\(2000\)001<0026:VAPOPA>2.0.CO;2](https://doi.org/10.1175/1525-7541(2000)001<0026:VAPOPA>2.0.CO;2).
- , P. A. Dirmeyer, A. N. Hahmann, R. Ijpelaar, L. Tyahla, P. Cox, and M. J. Suarez, 2002: Comparing the Degree of Land–Atmosphere Interaction in Four Atmospheric General Circulation Models. *J. Hydrometeorol.*, **3**, 363–375, [https://doi.org/10.1175/1525-7541\(2002\)003<0363:CTDOLA>2.0.CO;2](https://doi.org/10.1175/1525-7541(2002)003<0363:CTDOLA>2.0.CO;2).
- , and Coauthors, 2004: Realistic Initialization of Land Surface States: Impacts on Subseasonal Forecast Skill. *J. Hydrometeorol.*, **5**, 1049–1063, <https://doi.org/10.1175/JHM-387.1>.

- , and Coauthors, 2006: GLACE: The Global Land–Atmosphere Coupling Experiment. Part I: Overview. *J. Hydrometeorol.*, **7**, 590–610, <https://doi.org/10.1175/JHM510.1>.
- Koster, R. D., S. D. Schubert, and M. J. Suarez, 2009: Analyzing the Concurrence of Meteorological Droughts and Warm Periods, with Implications for the Determination of Evaporative Regime. *J. Clim.*, **22**, 3331–3341, <https://doi.org/10.1175/2008JCLI2718.1>.
- , and Coauthors, 2010: Contribution of land surface initialization to subseasonal forecast skill: First results from a multi-model experiment. *Geophys. Res. Lett.*, **37**, 1–6, <https://doi.org/10.1029/2009GL041677>.
- , and Coauthors, 2011: The Second Phase of the Global Land–Atmosphere Coupling Experiment: Soil Moisture Contributions to Subseasonal Forecast Skill. *J. Hydrometeorol.*, **12**, 805–822, <https://doi.org/10.1175/2011JHM1365.1>.
- Kumar, S., and Coauthors, 2014: Effects of realistic land surface initializations on subseasonal to seasonal soil moisture and temperature predictability in North America and in changing climate simulated by CCSM4. *J. Geophys. Res. Atmos.*, **119**, 13,250–13,270, <https://doi.org/10.1002/2014JD022110>.
- , M. Newman, D. M. Lawrence, M.-H. Lo, S. Akula, C.-W. Lan, B. Livneh, and D. Lombardozzi, 2020: The GLACE-Hydrology Experiment: Effects of Land–Atmosphere Coupling on Soil Moisture Variability and Predictability. *J. Clim.*, **33**, 6511–6529, <https://doi.org/10.1175/JCLI-D-19-0598.1>.
- Levis, S., and W. Sacks, 2011: Technical descriptions of the interactive crop management (CLM4CNcrop) and interactive irrigation models in version 4 of the Community Land Model. 13pp.
<http://www.cesm.ucar.edu/models/cesm1.2/clm/CLMcropANDirrigTechDescriptions.pdf>.
- Li, F., Y. J. Orsolini, N. Keenlyside, M.-L. Shen, F. Counillon, and Y. G. Wang, 2019: Impact of Snow Initialization in Subseasonal-to-Seasonal Winter Forecasts With the Norwegian Climate Prediction Model. *J. Geophys. Res. Atmos.*, **124**, 10033–10048,

<https://doi.org/10.1029/2019JD030903>.

Lo, M.-H., and J. S. Famiglietti, 2013: Irrigation in California's Central Valley strengthens the southwestern U.S. water cycle. *Geophys. Res. Lett.*, **40**, 301–306, <https://doi.org/10.1002/grl.50108>.



Lorenz, R., and Coauthors, 2016: Influence of land-atmosphere feedbacks on temperature and precipitation extremes in the GLACE-CMIP5 ensemble. *J. Geophys. Res. Atmos.*, **121**, 607–623, <https://doi.org/10.1002/2015JD024053>.

Lu, Y., K. Harding, and L. Kueppers, 2017: Irrigation Effects on Land–Atmosphere Coupling Strength in the United States. *J. Clim.*, **30**, 3671–3685, <https://doi.org/10.1175/JCLI-D-15-0706.1>.

Mahanama, S., B. Livneh, R. Koster, D. Lettenmaier, and R. Reichle, 2012: Soil Moisture, Snow, and Seasonal Streamflow Forecasts in the United States. *J. Hydrometeorol.*, **13**, 189–203, <https://doi.org/10.1175/JHM-D-11-046.1>.

Manabe, S., 1969: Climate and the Ocean Circulation. Part I: the Atmospheric Circulation and the Hydrology of the Earth's Surface. *Mon. Weather Rev.*, **97**, 739–774, [https://doi.org/10.1175/1520-0493\(1969\)097<0739:CATOC>2.3.CO;2](https://doi.org/10.1175/1520-0493(1969)097<0739:CATOC>2.3.CO;2).

Materia, S., A. Borrelli, A. Bellucci, A. Alessandri, P. DiPietro, P. Athanasiadis, A. Navarra, and S. Gualdi, 2014: Impact of Atmosphere and Land Surface Initial Conditions on Seasonal Forecasts of Global Surface Temperature. *J. Clim.*, **27**, 9253–9271, <https://doi.org/10.1175/JCLI-D-14-00163.1>.

Maupin, M. A., J. F. Kenny, S. S. Hutson, J. K. Lovelace, N. L. Barber, and K. S. Linsey, 2014: Estimated use of water in the United States in 2010. *U.S. Geological Survey*, Circular 1405, 56 pp.

McDermid, S. S., C. Montes, B. I. Cook, M. J. Puma, N. Y. Kiang, and I. Aleinov, 2019: The Sensitivity of Land–Atmosphere Coupling to Modern Agriculture in the Northern Midlatitudes. *J. Clim.*, **32**, 465–484, <https://doi.org/10.1175/JCLI-D-17-0799.1>.

- McGuire, V., 2007: Water-level changes in the High Plains aquifer, predevelopment to 2005 and 2003-2005. *US Geological Survey Scientific Investigations*, Rep. 2006-5324, 7 pp.
- Moore, N., and S. Rojstaczer, 2001: Irrigation-Induced Rainfall and the Great Plains. *J. Appl. Meteorol.*, **40**, 1297–1309, [https://doi.org/10.1175/1520-0450\(2001\)040<1297:IIRATG>2.0.CO;2](https://doi.org/10.1175/1520-0450(2001)040<1297:IIRATG>2.0.CO;2).
- Oleson, K. W., and Coauthors, 2013: Technical Description of version 4.5 of the Community Land Model (CLM). NCAR/TN-503+STR.
- Oleson K.W., and Coauthors, 2010: Technical description of version 4.0 of the Community Land Model (CLM). 257pp.
- Orsolini, Y. J., R. Senan, G. Balsamo, F. J. Doblas-Reyes, F. Vitart, A. Weisheimer, A. Carrasco, and R. E. Benestad, 2013: Impact of snow initialization on sub-seasonal forecasts. *Clim. Dyn.*, **41**, 1969–1982, <https://doi.org/10.1007/s00382-013-1782-0>.
- Pan, Z., E. Takle, M. Segal, and R. Turner, 1996: Influences of Model Parameterization Schemes on the Response of Rainfall to Soil Moisture in the Central United States. *Mon. Weather Rev.*, **124**, 1786–1802, [https://doi.org/10.1175/1520-0493\(1996\)124<1786:IOMPSO>2.0.CO;2](https://doi.org/10.1175/1520-0493(1996)124<1786:IOMPSO>2.0.CO;2).
- Pei, L., N. Moore, S. Zhong, A. D. Kendall, Z. Gao, and D. W. Hyndman, 2016: Effects of Irrigation on Summer Precipitation over the United States. *J. Clim.*, **29**, 3541–3558, <https://doi.org/10.1175/JCLI-D-15-0337.1>.
- Peings, Y., H. Douville, R. Alkama, and B. Decharme, 2011: Snow contribution to springtime atmospheric predictability over the second half of the twentieth century. *Clim. Dyn.*, **37**, 985–1004, <https://doi.org/10.1007/s00382-010-0884-1>.
- Prodhomme, C., F. Doblas-Reyes, O. Bellprat, and E. Dutra, 2016: Impact of land-surface initialization on sub-seasonal to seasonal forecasts over Europe. *Clim. Dyn.*, **47**, 919–935, <https://doi.org/10.1007/s00382-015-2879-4>.
- Puma, M. J., and B. I. Cook, 2010: Effects of irrigation on global climate during the 20th century. *J. Geophys. Res.*, **115**, D16120, <https://doi.org/10.1029/2010JD014122>.

- Qian, Y., M. Huang, B. Yang, and L. K. Berg, 2013: A Modeling Study of Irrigation Effects on Surface Fluxes and Land–Air–Cloud Interactions in the Southern Great Plains. *J. Hydrometeorol.*, **14**, 700–721, <https://doi.org/10.1175/JHM-D-12-0134.1>.
- Quesada, B., R. Vautard, P. Yiou, M. Hirschi, and S. I. Seneviratne, 2012: Asymmetric European summer heat predictability from wet and dry southern winters and springs. *Nat. Clim. Chang.*, **2**, 736–741, <https://doi.org/10.1038/nclimate1536>.
- Rasch, P. J., and Coauthors, 2019: An Overview of the Atmospheric Component of the Energy Exascale Earth System Model. *J. Adv. Model. Earth Syst.*, **11**, 2377–2411, <https://doi.org/10.1029/2019MS001629>.
- Schickedanz, P. T., 1976: The effect of irrigation on precipitation in the Great Plains. *Illinois State Water Survey*, NSF-RANN, Grant GI 43871, 105 pp.
- Schubert, S. D., M. J. Suarez, P. J. Pegion, R. D. Koster, and J. T. Bacmeister, 2008: Potential Predictability of Long-Term Drought and Pluvial Conditions in the U.S. Great Plains. *J. Clim.*, **21**, 802–816, <https://doi.org/10.1175/2007JCLI1741.1>.
- Segal, M., Z. Pan, R. W. Turner, and E. S. Takle, 1998: On the Potential Impact of Irrigated Areas in North America on Summer Rainfall Caused by Large-Scale Systems. *J. Appl. Meteorol.*, **37**, 325–331, <https://doi.org/10.1175/1520-0450-37.3.325>.
- Sellers, P. J., 1997: Modeling the Exchanges of Energy, Water, and Carbon Between Continents and the Atmosphere. *Science (80-.)*, **275**, 502–509, <https://doi.org/10.1126/science.275.5299.502>.
- Seneviratne, S. I., D. Lüthi, M. Litschi, and C. Schär, 2006: Land–atmosphere coupling and climate change in Europe. *Nature*, **443**, 205–209, <https://doi.org/10.1038/nature05095>.
- , T. Corti, E. L. Davin, M. Hirschi, E. B. Jaeger, I. Lehner, B. Orlowsky, and A. J. Teuling, 2010: Investigating soil moisture–climate interactions in a changing climate: A review. *Earth-Science Rev.*, **99**, 125–161, <https://doi.org/10.1016/j.earscirev.2010.02.004>.
- , and Coauthors, 2013: Impact of soil moisture–climate feedbacks on CMIP5 projections: First results from the GLACE-CMIP5 experiment. *Geophys. Res. Lett.*, **40**, 5212–5217,

<https://doi.org/10.1002/grl.50956>.

Siebert, S., M. Kummu, M. Porkka, P. Döll, N. Ramankutty, and B. R. Scanlon, 2007: Global Map of Irrigation Areas version 4.0.1. <https://mygeohub.org/publications/8/2>.

Siebert, S., M. Kummu, M. Porkka, P. Döll, N. Ramankutty, and B. R. Scanlon, 2015: A global data set of the extent of irrigated land from 1900 to 2005. *Hydrol. Earth Syst. Sci.*, **19**, 1521–1545, <https://doi.org/10.5194/hess-19-1521-2015>.

Thomas, J. A., A. A. Berg, and W. J. Merryfield, 2016: Influence of snow and soil moisture initialization on sub-seasonal predictability and forecast skill in boreal spring. *Clim. Dyn.*, **47**, 49–65, <https://doi.org/10.1007/s00382-015-2821-9>.

Tuttle, S., and G. Salvucci, 2016: Empirical evidence of contrasting soil moisture-precipitation feedbacks across the United States. *Science (80-.)*, **352**, 825–828, <https://doi.org/10.1126/science.aaa7185>.

Wada, Y., and M. F. P. Bierkens, 2014: Sustainability of global water use: past reconstruction and future projections. *Environ. Res. Lett.*, **9**, 104003, <https://doi.org/10.1088/1748-9326/9/10/104003>.

Wei, J., and P. A. Dirmeyer, 2012: Dissecting soil moisture-precipitation coupling. *Geophys. Res. Lett.*, **39**, n/a-n/a, <https://doi.org/10.1029/2012GL053038>.

Welty, J., and X. Zeng, 2018: Does Soil Moisture Affect Warm Season Precipitation Over the Southern Great Plains? *Geophys. Res. Lett.*, **45**, 7866–7873, <https://doi.org/10.1029/2018GL078598>.